REPUBLIC OF TURKEY
ACIBADEM MEHMET ALİ AYDINLAR UNIVERSITY
INSTITUTE OF HEALTH SCIENCES

BASE EXCISION REPAIR CAPACITY IN NON-MUSCLE-INVASIVE BLADDER CANCER

Fatma Merve ANTMEN

MASTER THESIS

DEPARTMENT of MEDICAL BIOTECHNOLOGY

SUPERVISOR
Prof. Dr. Meltem MÜFTÜOĞLU

ISTANBUL - 2018

REPUBLIC OF TURKEY
ACIBADEM MEHMET ALİ AYDINLAR UNIVERSITY
INSTITUTE OF HEALTH SCIENCES

BASE EXCISION REPAIR CAPACITY IN NON-MUSCLE-INVASIVE BLADDER CANCER

Fatma Merve ANTMEN

MASTER THESIS

DEPARTMENT of MEDICAL BIOTECHNOLOGY

SUPERVISOR
Prof. Dr. Meltem MÜFTÜOĞLU

ISTANBUL - 2018

Program:	Medical Biotechnology
Thesis title:	Base Excision Repair Capacity in Non-Muscle-Invasive Bladder Cancer
Students' name and surname:	Fatma Merve Antmen
Date of defence	06 / 07 / 2018

This is to certify that I have examined this copy of master thesis. I have found that she prepared after fulfilling requirements specified in the associated legislations before the final examining committee whose signatures are below.

Jury president	Prof. Dr. Tanıl Kocagöz Acıbadem Mehmet Ali Aydınlar University	Sign
Supervisor of the thesis	Prof. Dr. Meltem Müftüoğlu Acıbadem Mehmet Ali Aydınlar University	Sign
Jury member	Prof. Dr. Batu Erman Sabancı University	Sign

This thesis has been approved by the above jury and it has been accepted by decision of Health Sciences Board of Directors.

Sign

Prof. Dr. Uğur Özbek
Director of the Institute
Acıbadem Mehmet Ali Aydınlar University

DECLARATION

I hereby declare that, this thesis has been written by me based on the data obtained in line with the scientific rules and ethical principles of responsible conduct of research. All information, data, comments, analyses have been collected and processed through scientific, academic writing style, and literature used have been duly shown by giving reference to the original sources in accordance with the publication ethics. I also announce and emphasize that I have not violated any rules secured by patent and copyrights whilst the conduct and writing of this research.

06.07.2018

Fatma Merve ANTMEN

ACKNOWLEDGEMENTS

I would like to express my deepest thanks and sincere gratitude to my supervisor Professor Meltem Müftüoğlu for providing me exquisite facilities to perform this thesis and sharing her scientific knowledge and experiences with patience. I would like to mention that this thesis could not be happen without her. I also would like to thank for her generous mentorship.

I greatly acknowledge Professor Ümit İnce from the Department of Pathology and Professor Ali Rıza Kural and Dr. Selçuk Keskin from the Department of Urology, Acıbadem University and Acıbadem Maslak Hospital for providing patients' tissues. Also, I would like to thank my Müftüoğlu group labmates for their help and support during this study.

Additionally, I would like to thank my dear husband Anıl Berkay Antmen for his love, always being there for me and believing in me. I am grateful to my mother Gülin Tansev, father Ali Esat Tansev, brother Ali Mert Tansev, sister-in-law Eda Tansev and niece Fatma Ela Tansev for giving me infinite morale, support and love.

TABLE OF CONTENTS

LIST OF ABBREVIATIONS

3-meA	3-methyladenine
3-meG	3-methylguanine
3’-dRP or 3’-PUA	3’-phospho-α,β-unsaturated aldehyde
3’-P	3’-phosphate group
5-hmU	5-hydroxymethyluracil
5-OH-Cyt	5-hydroxycytosine
5-OH-Ura	5-hydroxyuracil
5’-dRP	5’-deoxyribosephosphate
5’-P	5’-phosphate group
7-meA	7-methyladenine
8-OH-Gua or 8-oxoG	7,8-dihydro-8-oxoguanine
A	Adenine
AAG or MPG	Alkyladenine/methylpurine DNA glycosylase
AP	Apyrimidinic/apurinic
AP-1	Activator protein 1
APE1	Apurinic/apyrimidinic endonuclease 1
BC	Bladder cancer
BCG	Bacillus Calmette-Guérin
BER	Base excision repair
BSA	Bovine serum albumin
C	Cytosine
Cg	Cytosine glycol
DSBR	Double-strand break repair
DTT	Dithiothreitol
EDTA	Ethylenediaminetetraacetic acid
ERCC1	Excision repair cross complementing 1
ERCC2	Excision repair cross complementing 2
FapyAde	4,6-diamino-5-formamidopyrimidine
FapyGua	2,6-diamino-5-formamidopyrimidine

FEN1	Flap endonuclease 1
G	Guanine
G-25	Sephadex G25 resin
H_2O_2	Hydrogen peroxide
IR	Ionizing radiation
LigI	DNA ligase I
LigIII	DNA ligase III
LP-BER	Long-patch BER
Lys	Lysine
MBD4	methyl-CpG-binding domain glycosylase 4
MIBC	Muscle-invasive bladder cancer
MMR	Mismatch repair
MMS	Methyl methanesulfonate
mt-BER	Mitochondrial BER
mtAPE1	Mitochondrial APE1
MUTYH	MutY homolog DNA glycosylase
NEIL1	Nei endonuclease VIII-like 1
NEIL2	Nei endonuclease VIII-like 2
NEIL3	Nei endonuclease VIII-like 3
NER	Nucleotide excision repair
NF-κB	Nuclear factor kappa B
NLS	Nuclear localization signal
NMIBC	Non-muscle-invasive bladder cancer
nt	Nucleotide
NTHL1	Endonuclease III-like 1
$O_2^{\bullet -}$	Superoxide radical
OGG1	8-oxoguanine glycosylase 1
OH•	Hydroxyl radical
PAGE	Polyacrylamide gel electrophoresis
PCNA	Proliferating cell nuclear antigen
PNK	Polynucleotide kinase
pol β	DNA polymerase β

pol γ	DNA polymerase γ
pol δ	DNA polymerase δ
pol ε	DNA polymerase ε
Ref-1	Redox factor-1
RF-C	Replication factor-C
ROS	Reactive oxygen species
SAM	S-adenosylmethionine
SMUG1	Single-strand-selective DNA glycosylase 1
SNP	Single nucleotide polymorphism
SP-BER	Short-patch BER
SSB	Single-strand break
T	Thymine
T4 PNK	T4 polynucleotide kinase
TCC	Transitional cell carcinoma
TDG	Thymine DNA glycosylase
THF	Tetrahydrofuran
TLS	Translesion synthesis
TNM	Tumor-nodes-metastasis
TUR	Transurethral resection
U	Uracil
UDG	Uracil DNA glycosylase
Ug	Uracil glycol
UNG	Uracil DNA N-glycosylase
UV	Ultraviolet radiation
XPF	Xeroderma pigmentosum group F
XRCC1	X-ray cross-complementing 1
XTH	Escherichia coli exonuclease III

LIST OF FIGURES

LIST OF TABLES

SUMMARY

Bladder cancer (BC) is the ninth most frequently diagnosed cancer and non-muscle-invasive BC (NMIBC) occupies the majority of BCs at diagnosis. In the treatment of the disease, bladder tumors are surgically removed and adjuvant therapy subsequently continues with chemotherapeutic drugs. These chemotherapeutic drugs show their cytotoxic effects by generating several types of damages on DNA, including oxidative DNA damage. Base excision repair (BER) mechanism is the main mechanisms that plays role in repairing the damage of these drugs. Balance of BER capacity is crucial for ensuring genomic stability and preventing drug resistance. How the patients' BER capacity affects NMIBC is not known yet. Therefore, in this study, it was aimed to investigate key BER enzymes activities and overall BER capacity in patients diagnosed with NMIBC. In this study, the enzyme activities were measured dependent on radioactivity in patients' NMIBC and corresponding normal tissues by using substrates that are peculiar to each enzyme. As a consequence, high-grade NMIBC tissues have been shown to have enhanced overall BER capacity due to increased UDG, APE1 and Pol β activities. Furthermore, inter-individual variations in the BER capacity have been demonstrated. Thus, these findings suggest that the increased in BER capacity of NMIBC due to increased UDG, APE1 and/or Pol β activities can enhance the chemotherapeutic resistance to NMIBC and contribute to progression of NMIBC. Moreover, UDG, APE1 and/or Pol β can be used as a predictive, prognostic and therapeutic target for NMIBC. Furthermore, inter-individual variations in BER capacity may contribute to the development of personalized therapy approaches for NMIBC cases.

Keywords: APE1, base excision repair, bladder cancer, Pol β, UDG.

ÖZET

Kasa İnvaze Olmayan Mesane Kanserinde Baz Eksizyon Tamir Kapasitesi

Mesane kanseri en sık teşhis konulan dokuzuncu kanser türüdür ve mesane kanseri tanılarının çoğunu kasa invaze olmayan mesane kanseri (KİOMK) kapsamaktadır. Hastalığın tedavisinde mesane tümörleri cerrahi olarak çıkarılmaktadır ve sonrasında kemoterapötik ilaçlarla destekleyici tedaviye devam edilmektedir. Bu kemoterapötik ilaçlar, oksidatif DNA hasarı da dahil olmak üzere, DNA üzerinde çeşitli türlerde hasarlar oluşturarak sitotoksik etkilerini göstermektedir. Baz eksizyon tamir (BER) mekanizması, bu ilaçların hasarlarının tamirinde rol oynayan temel mekanizmadır. BER kapasitesinin dengesi genomik kararlılığın sağlanması ve ilaçlara karşı oluşturulan direncin önlenmesi için çok önemlidir. Hastaların sahip olduğu BER kapasitesinin KİOMK üzerindeki etkisi henüz bilinmemektedir. Bu nedenle, bu çalışmada KİOMK tanısı konan hastalarda BER mekanizmasında rol oynayan temel enzimlerin aktivitelerinin ve genel BER kapasitesinin araştırılması hedeflenmiştir. Bu çalışmada, her enzime özgü substratlar kullanılarak, hastaların KİOMK ve karşılık gelen sağlıklı dokularındaki enzim aktiviteleri radyoaktiviteye bağlı olarak ölçülmüştür. Sonuç olarak, yüksek dereceli KİOMK dokularında artmış UDG, APE1 ve Pol β aktiviteleri nedeniyle, yüksek dereceli KİOMK dokularının artmış genel BER kapasitesine sahip olduğu gösterilmiştir. Buna ek olarak, BER kapasitesinde ortaya çıkan bireyler arası varyasyonlar gösterilmiştir. Bu bulgular, artmış UDG, APE1 ve/veya Pol β aktiviteleri nedeniyle KİOMK'de artmış BER kapasitesinin KİOMK'ye karşı kemoterapötik direnci artırabileceğini ve KİOMK'nin ilerlemesinde payı olabileceğini öne sürmüştür. Buna ek olarak, UDG, APE1 ve/veya Pol β, KİOMK için prediktif, prognostik ve terapötik hedefler olarak kullanılabilir. Ayrıca, BER kapasitesindeki bireyler arası varyasyonlar KİOMK vakaları için kişiye özgü tedavi yaklaşımlarının geliştirilmesine katkıda bulunabilir.

Anahtar Sözcükler: APE1, baz eksizyon tamiri, mesane kanseri, Pol β, UDG.

1. INTRODUCTION AND AIM

Bladder cancer (BC) is the ninth most frequently diagnosed cancer and non-muscle-invasive BC (NMIBC) occupies the majority of BCs at diagnosis (1,2). The development of BC is associated with non-environmental and environmental factors exposure (3,4). The underlying mechanism of BC due to environmental risk factors is not known yet. Because the urinary system involves the excretion of toxins, the accumulation of toxins in the bladder contributes to generation of DNA damage and initiation of BC (4). Treatment of BC is composed of transurethral resection (TUR) of bladder tumor and requires adjuvant therapy involving local settlement of chemotherapeutic drugs such as mitomycin c, epirubicin, doxorubicin, gemcitabine or Bacillus Calmette-Guérin (BCG) (4,5,6). These chemotherapeutic drugs show their cytotoxic effect by alkylating DNA, forming DNA crosslinks, generating reactive oxygen species (ROS) which cause oxidative DNA damage and single strand breaks (SSBs) (6,7,8). The base excision repair (BER) is the major repair pathway for oxidative, alkylated and deaminated bases and SSBs (9). The balance of BER capacity in cells/tissues/organisms is very significant because it maintains genomic stability. In particular cancer cells enhanced BER capacity protect them against DNA damaging chemotherapeutic drugs induced cell death and thus decrease the efficacy of anticancer therapy by demonstrating drug resistance while inadequate BER capacity in cells may lead carcinogenesis (10). Furthermore, since each individual has inherently different BER capacity, determining BER capacity of patients is crucial for selection of the ideal therapy that enhances his or her life quality.

The purpose of this thesis is to determine the activities of key BER enzymes and overall BER capacity of tumors and corresponding normal tissues of NMIBC patients. Since NMIBC requires continuous surveillance and administration of adjuvant therapy in order to prevent recurrence, determining BER activity and capacity of NMIBC patients will help us to understand the resistance to chemotherapy and the progression of disease. In addition, it will contribute to the development of predictive, prognostic and therapeutic biomarkers for NMIBC patients. Additionally, identified BER activity and capacity of NMIBC patients

enlighten the personalized anticancer therapy approaches for NMIBC by revealing the inter-individual variations of BER pathway.

2. BACKGROUND INFORMATION

2.1. Bladder Cancer

BC is the ninth common urinary system diseases. There are 430000 new diagnosed, and approximately 150000 deaths per year in worldwide (1,2). Incidence rates differ according to sex, as BC is the 4th common cancer in males whereas 9th in females, and it is more prevalent in the developed countries (5). Epidemiological studies indicate that BC is greatly related with non-environmental and environmental factors exposure (3,4). The familial history, age, sex, ethnicity, body weight, and lifestyle constitute the non-environmental risk factors (4). The major environmental risk factor that causes BC is tobacco smoking (50% of BC). The other factors include work related exposure to aromatic amines, polycyclic hydrocarbons, arsenic, and analgesics with phenacetin (1,2,3). The mechanism that plays role in the development of BC after environmental risk factors exposure is not known yet. Since various toxins are discarded via the urinary system, the accumulation of them can occur in the bladder and initiates BC (4). It is being considered as bladder tissue becomes more vulnerable to carcinogens after exposure to environmental risk factors. These carcinogens give rise to the formation of DNA damage and by-products that accelerate carcinogenesis and advancement of BC (3). The genetic factors can also contribute to the development of the disease.

Tumors of BC are staged and graded according to extension to tissue layers (Tis – T4) as seen in Figure 1 (2) and cellular characteristics as low- and high-grade by the Tumor-Nodes-Metastasis (TNM) system and 2016 WHO, respectively (2,11). Tis represent the cancer cells that are growing in the most superficial layer, which is the urothelial layer and Ta denotes the tumors that are growing into the bladder lumen as papillary structures whereas T1, T2, T3 and T4 tumors show invasion to the connective tissue layer, muscle layers, fat layer, adjacent tissues and organs, respectively (12). Low-grade tumors demonstrate mostly ordered appearance involving some atypical cells that vary in shape and size and lacking of significant mitotic activity (11,13) while high-grade ones have completely disorganized appearance and structure (11).

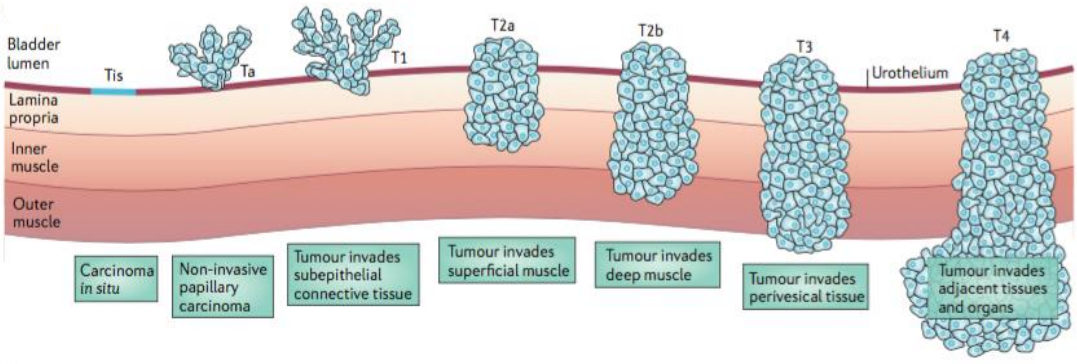

Figure 1. Stages of bladder cancer (2).

BCs comprehensively divided into two distinct groups: (i) NMIBC and (ii) muscle-invasive bladder cancer (MIBC) (5,14). As seen in Figure 1, NMIBC is composed of Ta and T1 stages whereas MIBC includes T2 to T4 stages (14). NMIBC patients undergo TUR of bladder tumor and require surveillance and adjuvant therapy including local settlement of chemotherapeutics such as mitomycin c, epirubicin, doxorubicin, gemcitabine or BCG according to pathological conditions (5,6). These chemotherapeutic agents demonstrate their cytotoxic effects by alkylating DNA, forming DNA crosslinks, oxidative DNA damage, and then lead to cell death (7). BCG is used as an immunomodulator that activates inflammatory responses (6). In addition to BCG's immunomodulator activity, it has been demonstrated that BCG treatment causes generation of ROS in urothelial cancer cells (8). In a long period of time, certain doses of adjuvant therapies are needed for patients that makes BC is a severe disease. NMIBC occupies approximately 70% to 80% of newly diagnosed BCs and in spite of the several therapies it shows recurrence about 50% to 70% and 1 out of 5 patients will show progress a MIBC (2,5,6,14). In addition, NMIBC patients five-year survival rate is accepted as about 90% whereas MIBC patients have five-year survival rate is lower than 50% and they show metastasis (2,14). The most commonly used treatment approach for MIBC patients are radical cystectomy and conventional chemotherapy with cisplatin and in addition to these therapies there is a need of multimodality therapy (6). For this reason, BC patients should be under constant follow up by cystoscopy and urine cytology that makes the disease one of the most expensive cancers due to the

requirement of continuous care from the diagnosis and therapy. Therefore it affects patient's life quality and economic conditions (2,6,15).

Although the TNM classification and definition of BC and their related therapy approach, the patients who have similarly staged show considerable heterogeneity in terms of treatment response and progression of the disease (15). In addition to this situation and also considering recurrence risk, which is the main problem for NMIBC, there is a vital need of biomarkers characterization to diagnose BC at an early stage, choose the ideal treatment condition for the patient, observe recurrence, clarify prognostic evaluations, estimate treatment response of the patient (14,15). As well as, characterization of that kind of biomarkers contributes to BC pathogenesis comprehension, improvement of the existing medication and therapy strategies, and development of new treatment and control strategies.

2.2. The DNA Damage and Its Effects

The human genome is continuously under the attack of exogenous and endogenous welded agents. It is estimated that approximately 10^5 DNA lesions per day are formed in a mammalian cell genome (16). Exogenous sources of DNA damage consist of ultraviolet (UV), X-rays, dietary factors, drugs, and environmental chemicals. Its endogenous sources include by-products of normal metabolism, chemical instability like depurination and depyrimidination, spontaneous errors such as mismatches, insertions and deletions during DNA replication (17,18). For example, the formation of apyrimidinic/apurinic (AP) sites arise at a rate of approximately 10^4/cell/day (19,20). Moreover, alkylating agents such as methyl radicals produced by lipid peroxidation and endogenous methyl donor S-adenosylmethionine (SAM) can cause alkylating DNA damage (19,21).

The unrepaired DNA damage can disrupt the normal processing of the cell that leads to genomic instability, apoptosis or senescence and as a consequence have effects on the organism's development and ageing (18,19). In addition to these, the organism that bears genomic instability gives tendency to immunodeficiency, neurological disorders and cancer (18). Therefore, cells have several DNA repair mechanisms to tolerate and repair different types of DNA lesions to maintain the genomic integrity and the stability of the organism (20).

2.2.1. Oxidative DNA damage

DNA can incur chemical modifications due to the oxidative damage that is a result of formation of reactive molecules. The most common type of these molecules is ROS (16). Endogenous welded ROS are produced mostly as by-products of mitochondrial oxidative phosphorylation and also produced due to the metabolism of several toxic agents and inflammatory response. They include superoxide radical ($O_2^{\bullet -}$), hydroxyl radical ($OH^{\bullet}$), and hydrogen peroxide (H_2O_2) (16,19). Exogenous welded ROS includes ionizing radiation (IR) and chemical agents like chemotherapeutic drugs (16). DNA, lipids and proteins are the potential targets for oxidative damage. When the proteins and lipids incur oxidative damage they can be replaced but oxidative DNA damage requires repair and if it left unrepaired, mutagenic DNA lesions occur (22). It is anticipated that ROS produce approximately 50000 lesions/cell/day, including oxidized deoxyribose, deaminated base products, and SSBs (Figure 2) (16,17,19,22). The BER pathway mainly cuts out these oxidative DNA lesions and maintain genomic integrity and stability (22,23).

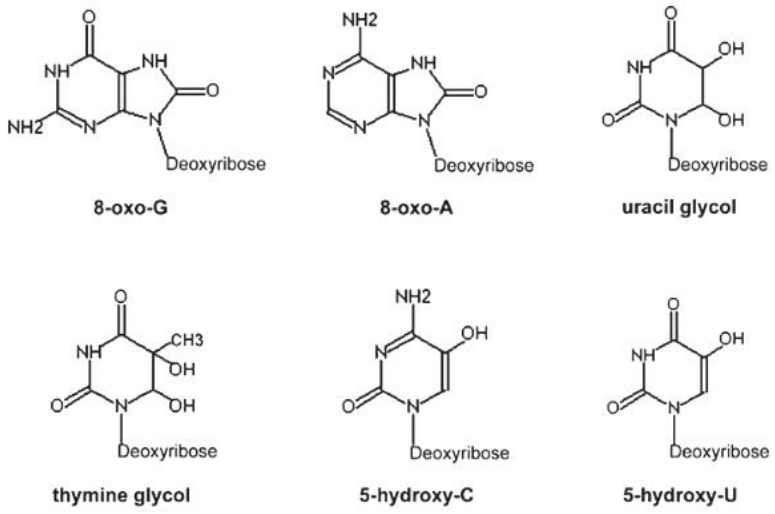

Figure 2. DNA base products caused by oxidative DNA damage (24).

The oxidative DNA damage by ROS is based on the principle of addition and abstraction. Mainly, $OH^{\bullet}$ removes an H atom from thymine (T)`s methyl group and generates several distinct types of final damaging products (22). Among these oxidized bases, 7,8-dihydro-8-oxoguanine (8-OH-Gua or 8-oxoG) is the most

common oxidative DNA lesion in organisms. It is highly mutagenic that mispairs with adenine (A) and thus leads to G:C to T:A transversions (19,22). It is considered as, under normal conditions, 8-OH-Gua is produced at a frequency of minimum of several hundred lesions per cell in each day because of the endogenous ROS (25). Deamination of exocyclic amino groups of the DNA bases due to oxidative stress is the other critical hydrolysis reaction that generates uracil (U) from cytosine (C). It is the most commonly formed DNA lesion due to deamination and it is considered as at a range of 100 to 500 per cell in each day (19). When the deamination of oxidized products of cytosine occurs, uracil-derived lesions are formed in DNA. For instance, deamination of cytosine glycol produce uracil glycol (Ug), 5-hydroxycytosine (5-OH-Cyt) and 5-hydroxyuracil (5-OH-Ura) (22) listed in Figure 2. Among the pyrimidine-derived lesions, 5-OH-Ura is potentially mutagenic because of GC:AT transitions (21). In addition to U generation from C deamination, hypoxanthine and xanthine can form from A and guanine (G) deamination, respectively (19,22). Other important types of oxidatively modified bases are formamidopyrimidines, which are 4,6-diamino-5-formamidopyrimidine (FapyAde) and 2,6-diamino-4-hydroxy-5-formamidopyrimidine (FapyGua), that are oxidative adducts due to the hydroxyl attack on A and G, respectively. It can cause GC:CG transversions (21).

2.3. DNA Repair Mechanisms

In order to overcome various types of DNA lesions and maintain genomic stability cells have evolved several different DNA repair mechanisms. Each mechanism repairs a different set of lesions, but there is also overlap between DNA repair pathways (19,26). Cells have four main types of DNA repair mechanisms as seen in Table 1. These are BER, mismatch repair (MMR), nucleotide excision repair (NER), and double-strand break repair (DSBR). Deficient DNA repair mechanisms due to germline or sporadic mutations accelerate carcinogenesis (26).

Table 1. DNA repair pathways and DNA lesions (19,27).

Damaging Agent	Example	Repair Mechanism	Repair Pathway
ROS, X-rays, alkylating agents, spontaneous reactions	Oxidation (8-oxoG), U, AP site, SSBR	BER	Recognition, N-glycosidic bond cleavage, removal of sugar fragment, gap filling and ligation
Replication errors	A-G and T-G mismatches, insertion, deletion	MMR	Recognition, excision of the strand, gap filling by DNA synthesis
UV light, polyaromatic hydrocarbons	Bulky adducts (cyclobutane-pyrimidine dimer), interstrand crosslink	NER	Recognition, excision of DNA fragment, sequential repair synthesis, strand ligation
X-rays, IR, anti-tumor agents	Double strand break, interstrand crosslink	DSBR	Unwinding, alignment, ligation

2.3.1. BER in mammalian cells

From bacteria to humans, BER is a mechanism that is highly conserved and repairs the most common DNA lesions consist of oxidized, alkylated, deaminated, and hydrolyzed bases as well as SSBs to maintain genomic stability and integrity (28). BER is defined as a highly coordinated pathway that perform repair with several different enzymatic reactions occurring consecutively and occurs both in the nucleus and mitochondria (16,19,29) (Figure 3). As seen in Figure 3, the BER pathway can be explained in five main steps for both mitochondrial and nuclear BER: (i) DNA glycosylases recognize and cut out the damaged base, (ii) 3'-OH generation (3'-end cleaning) by AP-endonucleases (APE1), (iii) 5'-end cleaning by AP lyases commonly associated to many DNA glycosylases and DNA polymerases, (iv) DNA polymerases fill the gap and (v) DNA ligases seal the nick (20,23).

At first, a DNA glycosylase, which is specific to the DNA lesion recognizes and incises the N-glycosidic bond between the base and the deoxyribose sugar (28,30). DNA glycosylases are either monofunctional or bifunctional according to their AP-lyase activity (30). In the monofunctional DNA glycosylase case, after the incision

step, the resulting intact AP site is processed by human apurinic/apyrimidinic endonuclease 1 (APE1). APE1 cleaves the phosphodiester backbone resulting a SSB with 3'-OH and 5'-deoxyribosephosphate (5'-dRP) end (30,31). On the other hand, a bifunctional DNA glycosylase has also intrinsic AP-lyase activity (30). The AP-lyase activity can be performed by either β-elimination of the 3' phosphodiester bond resulting with 3'-phospho-α,β-unsaturated aldehyde (3'-PUA or 3'-dRP) and 5'-phosphate group (5'-P) or β,δ-elimination of the 3' and 5' phosphodiester bonds resulting with 3'-phosphate group (3'-P) and 5'-P termini, depending on the enzyme (16,30,31). Following the bifunctional DNA glycosylase that uses β-elimination, the 3'-PUA is cleaved by APE1. The bifunctional DNA glycosylase remove 3'-P by polynucleotide kinase (PNK) via β,δ-elimination, (16,28,30).

Further part of the BER pathway involves gap filling and ligation. The gap filling and ligation steps can be performed according to two different subpathways, which are short-patch BER (SP-BER) and long-patch BER (LP-BER) (19,29). In SP-BER, a single nucleotide gap is synthesized and ligated, but in LP-BER a gap of 2 to 10 nucleotides are synthesized and ligated (29). LP-BER requires several enzymes such as proliferating cellular nuclear antigen (PCNA), flap endonuclease 1 (FEN1), replication factor-C (RF-C) and DNA polymerases dependent on PCNA including polymerase ε (pol ε) or polymerase δ (pol δ) and polymerase β (pol β) are needed to complete repair (30). Thus it is considered as LP-BER takes place in proliferating cells whereas SP-BER takes place in non-dividing cells (16,29). The 80-90% of all BER is composed of SP-BER (19,27).

In SP-BER, pol β with its dRP lyase activity turns the 5'-dRP residue to a ligatable 5'-P and inserts a single nucleotide at the newly formed 3'-OH termini (16,30,31). After pol β, nick's ligation is succeeded by DNA ligase III (LigIII) and the scaffolding protein X-ray cross-complementing 1 (XRCC1) (19,29).

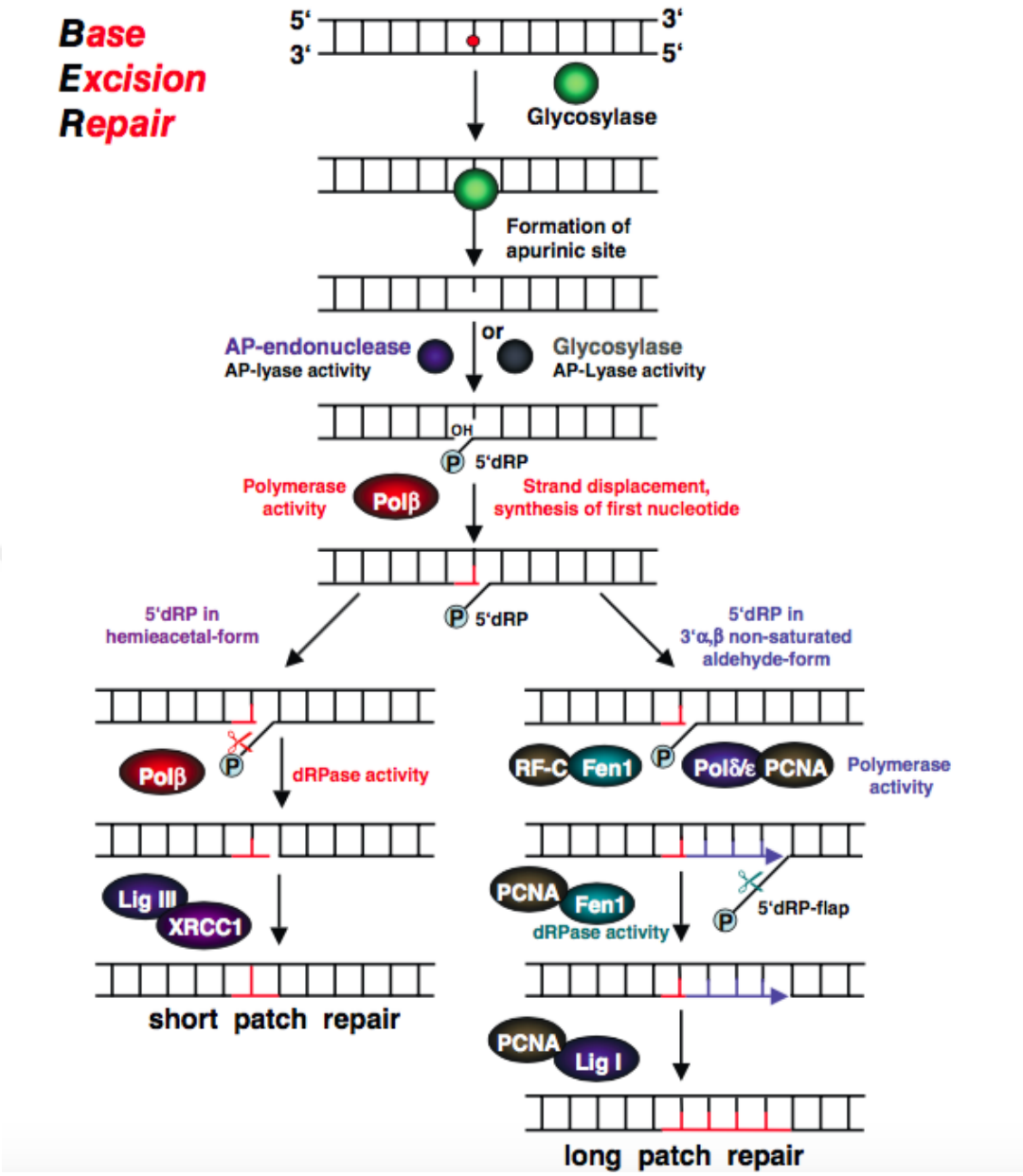

Figure 3. Detailed mechanism of base excision repair pathway (20).

XRCC1 stabilizes LigIII and their interaction enhances the ligation process (28,29). In LP-BER, pol β cannot exert its dRP lyase activity on AP sites and thus, the 5'-dRP termini cannot be removed and strand displacement is promoted (16,28). The PCNA dependent polymerases synthesize and displace 2 to 10 nucleotides downstream with the enhancement of PCNA and RF-C and a 5'-dRP overhang flap is generated (16). Then the removal of 5'-dRP overhang flap takes place via the

interaction of FEN1 and PCNA (16,20). After the removal of 5'-dRP overhang flap, by DNA ligase I (LigI) interacts with PCNA to seal the nick (20,28).

In mitochondrial BER (mt-BER), there are some minor differences are present. First one of those differences is the presence of polymerase γ (pol γ). At first it is estimated that only Pol γ exists in mt-BER and it has dRP lyase activity (32,33). However, a recent study demonstrated that pol β also participates in mitochondrial BER (34). The other difference occurs in the ligation step of mt-BER, LigIII is the essential ligase that takes place but interestingly it does not interact with XRCC1 (16,32).

2.3.1.1. DNA glycosylases

Currently, mammalian cells have 11 DNA glycosylases and each of them recognizes a defined group of DNA lesions as listed in Table 2 (29,30). Mitochondrial isoforms are not included in 11 DNA glycosylases since they are results of alternative splicing (29). DNA glycosylases are either monofunctional or bifunctional according to the catalytic mechanism that they have and the ability to perform AP lyase strand incision activity (35). Monofunctional DNA glycosylases have only glycosylase activity but in addition to glycosylase activity, bifunctional glycosylases have AP lyase activity (35,36). On the other hand, bifunctional DNA glycosylases execute phosphate backbone cleavage in addition to the N-glycosidic bond cleavage (30). They utilize β-elimination or β,δ-elimination to cleave the phosphate backbone and remove the damaged base (30,36). Both elimination reactions result with a DNA nick that is consist of a 3'-blocking termini (3'-PUA/3'-dRP) or 3'-P, respectively and those blocked 3'-termini's require further processing by specific enzymes for the completion of repair (35). Although DNA glycosylases have different structures and substrate selectivity, they share a common acting mechanism and they occur in three distinct conformations, which are the searching complex, the interrogation complex and the excision complex (30,36).

Table 2. Mammalian DNA glycosylases (28,30,35,36).

Type of the damaged base	Name of the glycosylase	Acronym	AP lyase activity	Substrates
Deaminated base	Uracil DNA glycosylase	UDG	No	U, U:G, U:A, 5-OH-Ura
	Thymine DNA glycosylase	TDG	No	U,T, 5-hmU, T:G
	Single-strand-selective DNA glycosylase 1	SMUG1	No	U, 5-hmU, U:A, U:G
	methyl-CpG-binding domain glycosylase 4	MBD4	No	T,U, and 5-hmU when paired with G in
Alkylated purines	Alkyladenine/methylpurine DNA glycosylase	AAG/MPG	No	3-meA, 7-meA, 3-meG, hypoxanthine
Oxidized base	MutY homolog DNA glycosylase	MUTYH	No	A:G, A:8-oxoG, A:FapyGua
	8-oxoguanine glycosylase 1	OGG1	Yes (β)	8-oxoG:C, FapyGua:C
	Endonuclease III-like 1	NTHL1	Yes (β)	Tg, Cg, FapyGua, 5-OH-Ura, 5-OH-Cyt
	Nei endonuclease VIII-like 1	NEIL1	Yes (β,δ)	Tg, Cg, FapyGua, 5-OH-Ura, 5-OH-Cyt, Urea, FapyAde, FapyGua
	Nei endonuclease VIII-like 2	NEIL2	Yes (β,δ)	Overlap with NTHL1 and NEIL1
	Nei endonuclease VIII-like 3	NEIL3	Yes (β,δ)	FapyGua, FapyAde

DNA glycosylases change conformation to the interrogation complex when they encounter an oxidized base and favor the damaged base to flip out of the DNA duplex into the substrate-binding region (30,36). In the presence of the damaged base in substrate-binding pocket of DNA glycosylases, the enzyme shifts its conformation to the excision complex and after this; the excision process is continued with each DNA glycosylase's respective mechanism (30).

Despite the fact that human DNA glycosylases have different substrate specificities, they often share overlapping specificities mostly in oxidative DNA damage repair (35). Basically, four out of the eleven human DNA glycosylases remove mispaired U and T, six of them take place in the repair of oxidized bases and only one of them removes alkylated bases. (28,35) The DNA glycosylases, which

take removes the deaminated and alkylated bases are belonging to the monofunctional group (28). However, except one, the DNA glycosylases specific for oxidized bases` repair are included in bifunctional DNA glycosylases (28,35).

U in the DNA is the most common lesion that exists in DNA due to C`s hydrolytic deamination or a replication mistake and thus, pairs with A leading to C:G to T:A transition (35). U and U-derived lesions are recognized and removed by uracil DNA glycosylase (UDG) superfamily composed of Uracil DNA glycosylase (UDG), thymine DNA glycosylase (TDG), single-strand-selective DNA glycosylase 1 (SMUG1), and methyl-CpG-binding domain glycosylase 4 (MBD4) (30,35).

The alkyladenine/methylpurine DNA glycosylase (AAG/MPG) is the only DNA glycosylase that removes the alkylated base lesions. These lesions are produced by chemotherapeutic agents and environmental chemicals etc. (28,35). There are several types of oxidatively modified base damages repaired by different types of DNA glycosylases which are MutY homolog DNA glycosylase (MUTYH), 8-oxoguanine glycosylase 1 (OGG1), endonuclease III-like 1 (NTHL1), Nei endonuclease VIII-like 1 (NEIL1), Nei endonuclease VIII-like 2 (NEIL2) and Nei endonuclease VIII-like 3 (NEIL3) listed in Table 2 (35).

The human *OGG1* gene produces α-OGG1 and β-OGG1 by alternative splicing (37). β-OGG1 present in mitochondria whereas α-OGG presents in both nucleus and mitochondria (38). Furthermore, the alternative splices products of *UNG* gene is UNG1 and UNG2. UNG1 exist in mitochondria and UNG2 exists in nucleus (37,38).

2.3.1.2. APE1

In DNA, AP sites occur due to N-glycosidic bond`s hydrolysis of DNA glycosylases (39). It is estimated that 10000 AP sites are formed per day commonly due to the loss of a purine (40). It is important to maintain AP site repair for genome stability because if it is not repaired, it can block DNA replication and transcription, promote both mutation and SSBs (30,39,41). The biological significance of APE1 is emphasized by identifying that the mammalian cells which lack APE1 shows embryonic lethality (30). However, another AP endonuclease that is apurinic/apyrimidinic endonuclease 2 (APE2) has been defined in human cells (37). Yet, it is identified that APE2's endonuclease activity is far lower than APE1 (40).

Human APE1 is produced by *APEX1* gene, which is approximately 3 kb in size and localized on 14q11.2 and composed of four introns and five exons (42,43). APE1 functions in BER, transcription, and cell proliferation (42). In BER, APE1 has two principal enzymatic activities: (i) incision of the phosphodiester backbone 5' in AP sites, resulting with a SSB and, (ii) 3'-dRP removal that is a result of β-elimination by bifunctional DNA glycosylases and creating 3'-OH substrates for DNA polymerases by showing its 3'-phosphodiesterase activity (30,37,40). Moreover, APE1 can also provide the coordination of steps of BER. It is established that APE1 boosts DNA glycosylase-product complex dissociation and by this way increases the multiple turnover rates of DNA glycosylases such as UDG, AAG, TDG, and OGG1 (40,42). Two mechanisms have been introduced to clarify this situation: a passive mechanism and an active mechanism. Passive mechanism is based on the cleavage of the AP site that prevents rebinding of DNA glycosylase whereas active mechanism displaces DNA glycosylase from the AP site directly (42). APE1 promotes 5'-dRP excision activity of pol β and shows proofreading for pol β via its 3'-5' exonuclease activity (40,44). APE1's endonuclease activity is based on a nucleophilic attack of an activated water molecule's hydroxide ion on the 5'-P of the AP site (31,40). Also for the catalytic activity of APE1, divalent cations such as Mg^{2+} or Mn^{+2} are required (33,42). Mg^{2+} are required for both DNA binding and phosphodiester bond incision of APE1, so it is defined, as the limiting step of the reaction is dependent on the Mg^{2+} concentration (40). Furthermore, APE1 is described as a redox factor-1 (Ref-1) apart from its endonuclease and exonuclease activities (40,43). As Ref-1, APE1 coordinates gene expression by stimulating DNA-binding activity of certain transcription factors such as activator protein 1 (AP-1) and nuclear factor kappa B (NF-κB) (43). It is importantly indicated that oxidation of cysteines via ROS constrains AP-1`s DNA binding activity and to overcome this situation Ref-1 reduces these cysteine residues via the redox mechanism and thus, activates AP-1 (42). Additionally, Ref-1 enhances p53's DNA-binding ability, promotes transcriptional activation of p53 target promoters, and takes place in the regulation of the p53's proapoptotic functions (40).

The human APE1 protein has sequence homology with Escherichia coli exonuclease III (xth) but differently, it possesses a unique N-terminal domain (43).

APE1's endonuclease domain is involved in phosphoesterase superfamily of enzymes that possess a four-layered α/β sandwich structural core and changeable loop regions and active site specialties that ensures substrate specificity and sliding along the strand to search of an AP site by interacting with the DNA backbone. The stabilization of the AP site and the APE1:DNA complex is provided by the loop domains which interact the minor and major grooves at the AP site and 5'- or 3'-region of the AP site, respectively (30). It is established that the N-terminal domain is independent of the APE1's DNA repair functions (40). In a recent study, it has been showed that the deletion of the first 61 amino acid residues in APE1 (APE1-NΔ61) reduces its redox activity but has a proficient AP cleavage site activity similar to the full-length APE1 protein. However, it has been also indicated that APE1-NΔ61 cannot promote the multiple turnover of DNA glycosylases OGG1, MBD4, and AAG in contrast to full-length APE1 and therefore, it is proposed that the N-terminal of APE1 which possesses redox activity provides interactions with DNA and the occurring conformational changes due to APE1 binding is involved in the disruption of the DNA glycosylase-AP site DNA complex (42). Additionally, APE1 contains a nuclear localization signal (NLS) in its N-terminal domain, and depending on the cell type APE1 predominantly occurs in the nucleus. However, in the mitochondrial extracts AP site cleavage activity is also detected and mitochondrial APE1 (mtAPE1) has been described as a truncated protein devoid of the N-terminal domain of 33 amino acid residues, containing NLS (38,40).

2.3.1.3. DNA polymerase β (Pol β)

Pol β is 39-kDa DNA polymerase coded by the *POLB* gene spanning 33 kb and located on 8p11.21 in humans, and composed of thirteen introns and fourteen exons (45,46). It has been established that Pol β is composed of two distinct domains that each has a specific catalytic activity: the amino-terminus 8-kDa and the carboxyl-terminal 31-kDa polymerase domains (45,47,48). It has been showed that DNA Pol β primarily takes place in BER (47). In the BER pathway, Pol β comes after APE1 and shows two catalytic activities: (i) converting the 5'-dRP residue to a 5'-P via its intrinsic dRP lyase activity resulting with formation of a one-nucleotide gap and (ii) synthesis of a single nucleotide to the 3'-OH of the nick (31,45). The nucleotidyl transferase activity comes from the 31-kDa polymerase domain whereas

the amino-terminus 8-kDa domain has the dRP lyase activity (48). The lack of *Pol β* gene in a mouse model system eventuated with embryonic lethality whereas cultured embryonic mouse fibroblasts are viable but show accumulation of cytotoxic repair intermediates that leads hypersensitivity to genomic toxicants (45,48). Pol β also interplays with other BER factors including APE1, DNA ligase and XRCC1 which accelerates repair, besides its direct enzymatic activities (45,47). In addition to Pol β's dRP lyase activity, the 8-kDa domain contains single strand binding activity which leads the enzyme to bind 5'-P or 5'-dRP that occurs in gapped DNA (45). The dRP lyase reaction produces a 5'-P and its characterization shows that it is critically more rapid than one nucleotide incorporation and thus, it is estimated as the 8-kDa domain of Pol β coordinates the DNA synthesis (45,47). The 5'-P binds to the lyase domain via forming hydrogen bonds with Lys35 and Lys68. For the removal of the 5'-dRP residue, Lys72 acts as a nucleophile (45). Pol β's polymerase domain contains three subdomains that each has distinct functions: the C-subdomain, the D-subdomain and the N-subdomain (45,48). C-subdomain requires Mg^{+2} to perform nucleotidyl transferase activity while the D-subdomain and N-subdomain play role in binding duplex DNA and nascent base pair (dNTP and templating nucleotide), respectively (31,45,48). The binding of Pol β to the DNA backbone of the incised DNA strand is ensured by the helix-hairpin-helix motif and Na^{+} binding to perform further interactions for both the lyase domain and the D-subdomain (45).

To date, in mt-BER, Pol γ is the main DNA polymerase. However, recent study indicated that Pol β exists in mitochondrial protein extracts derived from mammalian tissue and cells suggesting that a cleavage or disruption may occur in the N-terminal NLS resulting with mitochondrial localization (34).

2.4. The Relationship between BER and Cancer

Oxidative DNA damage is one of the factors that lead to cancer development. The unrepaired DNA damage may lead formation of mutations and chromosomal instabilities that affects oncogenes and tumor suppressor genes resulting with carcinogenesis (49). Therefore, there is a critical link between the cancer growth and the function of DNA repair enzymes and the oxidative stress that is causing damage (30). In addition to the direct link between the DNA repair capacity and the risk of

cancer development, there is another relation between the DNA repair capacity's effects on the cancer patient's response to cancer therapy. In that perspective, decreased DNA repair capacity is undesirable because of the potential to develop cancer whereas, especially in tumor cells the increased DNA repair capacity is undesirable due to the formation of resistance to DNA damaging therapeutics (10). Thus, selective inhibiting of DNA repair enzymes is promising when combined with currently used chemotherapeutic agents and radiation to overcome drug resistance (50,51).

BER is the key pathway that is considered in the therapeutic approach in cancer since it is responsible for repairing small not-distorting DNA lesions like oxidized or alkylated bases and SSBs that are formed during cell metabolism as well as produced by chemotherapeutic agents in cancer therapy (51,52). Another reason to target BER pathway is the condition that cancer cells are in a higher oxidative state than the normal cells due to high ROS generation during increased metabolism and tumor microenvironments promoting more oxidative stress. As a consequence, cancer cells are expose to more oxidative damage and requires BER to overcome DNA damage to sustain cellular survival (52,26). At the beginning of BER, DNA glycosylases cut out the damaged base. It is denoted that DNA glycosylase knockout mice develop normally in spite of the accumulation of lesions in DNA and does not show significant increase in cancer initiation rates (53). The reason for that may be the overlapping substrate specificity of DNA glycosylases and the ability to correctly replicate via lesion bypass polymerases (50,53). On the other hand, in several studies it has been mentioned that down regulation of *OGG1* gene and low OGG1 activity is a risk factor in the development of lung, head and neck cancers (54,55). However, it is also denoted that overexpression of OGG1 mRNA for the excision of 8-oxoG has been detected in several lung cancer cell lines in compared to control lung cell lines (54). Furthermore, colorectal cancer patients show increased OGG1 mRNA levels and higher 8-oxoG excision than healthy people, indicating that enhanced DNA repair capacity present in colorectal cancer patients (56). It is suggested that overexpression of DNA glycosylases in cancer cells may lead to drug resistance (53). $UNG^{-/-}$ colon cancer cells have been shown to hyper-sensitization to pemetrexed, which is a chemotherapeutic drug (57). In another study it has been indicated that,

OGG1 deficient lung cancer cells showed enhanced sensitivity and reduced cellular resistance to bleomycin that is a chemotherapeutic agent (58).

APE1 is one of the most important enzymes take place in BER. Beside of its role in BER, APE1 has a role in regulating transcription factors, cell proliferation and cell response to oxidative stress. Thus, complete knocking down of APE1 is not possible for both cancer and normal cell survival (51). Several studies have demonstrated that APE1 is overexpressed in various cancer types such as prostate, breast, triple-negative breast, colon, ovarian, non-small cell lung, head and neck squamous cancers (55,56,59-64). It is indicated that the overexpression of APE1 is associated with resistance to chemotherapy and radiotherapy (53,65). Moreover, down regulation and inhibition of APE1 function in ovarian, non-small cell lung and triple-negative breast cancer types increase sensitivity of chemotherapeutic drugs such as cisplatin, camptothecin and olaparib (61-64). As a consequence, APE1 is attracting attention to design a novel therapy based on a specific inhibition of its endonuclease and redox activity that increase cancer cells sensitivity to chemotherapeutic agents and radiotherapy (40,51).

Pol β is the major DNA polymerase involved in BER pathway that has a low fidelity and an ability to perform translesion synthesis (TLS) (53,66). Overexpression and aberrant forms of Pol β has been associated with multiple cancer types such as breast, ovarian, colon, prostate, esophageal and colorectal cancers (66-71). A recent study demonstrated that higher expression levels of Pol β is related with tumor metastasis and poor prognosis in esophageal cancer patients (71). Another study established that colorectal cancer patients with higher levels of Pol β show poorer survival (69). It has been also mentioned that elevated expression of Pol β is detected in drug-resistant cells (66). It has been determined that increased activity and expression of Pol β exist in cisplatin resistant human ovarian tumor cells (70). Moreover, a very recent study determined that Pol β deficient gastric cancer cells show sensitivity to methyl methanesulfonate (MMS), which is an alkylating agent, used in chemotherapy approaches (72). These data indicate that diversification of Pol β's expression and composition contribute mutagenesis, genomic instability and carcinogenesis by interfering with BER pathway (67,73). It has been indicated that Pol β can bypass the DNA lesions which are the products of chemotherapeutic agents

(66). Overexpression and increased activity may cause enhances TLS ability in addition to mutagenesis and contribute cancers cells capability to overcome the highly stressed environment which exists due to increasing replication rates and higher levels of oxidative damage. Therefore, increased TLS capability could also results with chemotherapeutic drug resistance (68).

All these facts propose that understanding the functional situation of BER proteins and determining BER capacity of tumors are critical for predictive, prognostic and therapeutic approaches for cancer (54,73).

2.4.1. The relationship between BER and NMIBC

DNA repair pathways affect tumor behavior and response to treatment. Since the chemotherapeutic agents used in BC treatment are function by inducing oxidative stress, variations in genes and their products involved in oxidative stress response pathways such as BER pathway have a significant role in treatment approaches (74).

In the literature, most of the studies have established a relationship between BC with NER pathway. It is indicated that low expression level of a NER gene which is excision repair cross complementing 1 (ERCC1) is associated with enhanced oxidative stress and low ERCC1 mRNA expression levels correlate with longer median survival in advanced stage BC patients who received cisplatin-based chemotherapy (75). Therefore, it is suggested that as the DNA repair capacity increases by ERCC1 expression, the chemosensitivity decreases (74,75). Moreover, a recent study has been demonstrated an association between mutations of excision repair cross complementing 2 (*ERCC2*) gene that plays role in NER and response to cisplatin-based chemotherapy and hypothesized that the mutations resulting with loss of normal ERCC2 function drive enhanced tumor cell sensitivity to DNA damaging agents like cisplatin (76). In another study, it is denoted that BC tissues that are exposed to a chemotherapeutic agent hydroxycamptothecin have significantly higher mRNA expression and protein levels of xeroderma pigmentosum group F (XPF), which forms a complex with ERCC1 during NER, than chemotherapy-naïve BC tissues (77).

In the context of BER pathway it is important to consider the oxidative stress condition of patients. In a very recent study, serums of the BC patients are analyzed

and it is determined that the patients total oxidant statuses are significantly higher and total antioxidant statuses are significantly lower than the healthy people (78). Hence, it is critical to investigate BC in the context of BER pathway. In the literature, there are several studies present that seek a relation between BC and polymorphisms of BER genes (9,67,79,80). For instance, five single nucleotide polymorphisms (SNPs) in *NEIL2* gene are determined as significantly associated with disease recurrence of BCG-treated NMIBC patients while one SNP in *UDG* gene is found as associated with NMIBC progression (81). Another study has been revealed a SNP in *SMUG1* gene that is significantly associated with BC risk while one SNP of Pol β conferred higher BC risk (9). A recent meta-analysis has been mentioned that there is no significant relation between *OGG1* gene polymorphisms and BC risk (82). On the other hand, three SNPs in *XRCC1* gene has been mentioned as associated with the increased recurrence risk in BC cancer patients who treated with BCG (83). As well as genetic variants, it has been demonstrated that the tumors of MIBC patients treated with radical radiotherapy having higher APE1 and XRCC1 protein expression levels are associated with improved cancer-specific survival (84). One of the recent studies has been denoted that high-grade tumors of patients diagnosed with urothelial carcinoma of bladder showed increased levels of APE1, XRCC1 and Pol β in compared with low-grade tumors and, also it is found out that poor clinical outcome was associated with reduced levels of APE1 at initial diagnosis regardless of the pathological grade, stage or therapeutic approach (85). In addition to these findings, there are a few studies indicating that the elevated levels and expression of APE1/Ref-1 protein exist in serum and urine of NMIBC and MIBC patients and its level is found associated with the severity of the disease (86,87). However, there is no any finding comprising the activity of enzymes responsible for BER in the context of NMIBC.

All these facts emphasize the need of determining the activities of BER enzymes to choose the best treatment approach that the patient will benefit most that avoid poor clinical outcomes and overcome drug resistance.

3. MATERIALS AND METHODS

3.1. NMIBC and Corresponding Normal Tissues

Seventeen NMIBC tumor and their corresponding non-cancerous tissues were received from Urology Department at Acıbadem Maslak Hospital (Istanbul, Turkey) by cold cup biopsy before TUR. Following TUR, fresh tissues were snap-frozen, and stored in liquid nitrogen. Evaluation and gradation of NMIBC tumor and corresponding normal tissues were done by the Pathology Department of Acıbadem Maslak Hospital (Istanbul, Turkey) according to the previously published criteria (88). All NMIBC patients were newly diagnosed, and had not been treated with BCG, chemotherapy or radiotherapy at the time of TUR. Of the seventeen NMIBC patients, fourteen were men and three were women as seen in Table 3. All NMIBC tumors belong to this study were classified as high-grade and low-grade transitional cell carcinoma (TCC). Before participation in this study, written informed consents were received from all NMIBC patients. The study was approved by the Ethical Committee of Acibadem Mehmet Ali Aydinlar University and Acibadem Health Institutions Medical Research (ATADEK).

Table 3. Characteristics of the patients.

Characteristics	Data
Number of patients with primary tumor diagnosis	17
Mean age (years)	68
Gender, n (%)	
Female	3 (18)
Male	14 (82)
Grade, n (%)	
Low-grade	6 (35)
High-grade	11 (65)
Stage, n (%)	
Ta/T1	17 (100)

3.2. Whole Tissue Lysate Preparation

Whole tissue lysate preparations were done according to previously described protocol (89) with some alterations. At the beginning of this study, all of the tissues were homogenized in ice-cold MSHE buffer including 210 mM mannitol, 70 mM sucrose, 10 mM HEPES, 1 mM EGTA, 2 mM EDTA, 0,15 mM spermine, 0,75 mM spermidine, 5 mM DTT and 1xcomplete^{TM} protease inhibitor tablet (Roche Applied Sciences, USA) with using a dounce glass-glass homogenizer. Then the tissue homogenate was centrifuged at 16000xg for 15 minutes at 4°C. The pellet was dissolved by using one volume of buffer I containing 10 mM Tris-HCl (pH 7.8) and 200 mM KCl, and two volumes of buffer II containing 10 mM Tris-HCl (pH 7.8), 200 mM KCl, 2 mM EDTA, 40% glycerol, 1 mM PMSF, 0.2% NP-40, 2 mM DTT and 1xcomplete^{TM} protease inhibitor tablet (Roche Applied Sciences, USA). Immediately after dissolving the pellet, sonication was applied to fragmentize DNA. The lysates were rocked for 2 hours at 4°C. The lysates were centrifuged at 130000xg for 1 hour at 4°C. The supernatant was dialyzed at 4°C and left overnight in buffer III (dialysis buffer) containing 25 mM HEPES-KOH (pH 7.5), 100 mM KCl, 1 mM EDTA, 1 mM DTT, 15% glycerol, 12 mM $MgCl_2$. After overnight incubation, the cell lysates were centrifuged at 16000xg for 10 minutes at 4°C to remove insoluble particles. Afterwards, the lysates were snap-frozen in liquid nitrogen and stored at -80°C. Protein concentration of the lysates was determined by the Bradford protein assay (Bio-Rad, USA) and bovine serum albumin (BSA; Bio-Rad, USA) was used as a standard. The measurement was taken by PowerWave™ XS2 microplate spectrophotometer (BioTek, USA) at 595 nm.

3.3. Oligodeoxynucleotides

To understand the repair pathways of modified DNA bases, synthetic single lesion oligodeoxynucleotides have been used. The sequences of the oligonucleotides are listed in Table 4. All oligodeoxynucleotides were purchased from DNA Technology, Denmark.

Table 4. The sequence of oligodeoxynucleotides used in this study.

Oligodeoxynucleotides and Sequences
1st-25mer 5’-GCTTAGCTTGGAATCGTATCATGTA-3’
2nd-25mer 5’-ACTCGTGTGCCGTGTAGACCGTGCC-3’
Uracil (U) 5’-GCTTAGCTTGGAATCGTATCATGTA**U**ACTCGTGTGCCGTGTAGACCGTGCC-3’ 3’-CGAATCGAACCTTAGCATAGTACATGTGAGCACACGGCACATCTGGCACGG-5’
X=Tetrahydrofuran (THF) 5’-GCTTAGCTTGGAATCGTATCATGTA**X**ACTCGTGTGCCGTGTAGACCGTGCC-3’ 3’-CGAATCGAACCTTAGCATAGTACATGTGAGCACACGGCACATCTGGCACGG-5’
8-oxoguanine (8-oxoG) 5’-GCTTAGCTTGGAATCGTATCATGTA**OH G**ACTCGTGTGCCGTGTAGACCGTGCC-3’ 3’-CGAATCGAACCTTAGCATAGTACAT GTGAGCACACGGCACATCTGGCACGG-5’
1nt-Gap 5’-GCTTAGCTTGGAATCGTATCATGTA ACTCGTGTGCCGTGTAGACCGTGCC-3’ 3’-CGAATCGAACCTTAGCATAGTACATGTGAGCACACGGCACATCTGGCACGG-5’
Control 5’-GCTTAGCTTGGAATCGTATCATGTACACTCGTGTGCCGTGTAGACCGTGCC-3’ 3’-CGAATCGAACCTTAGCATAGTACATGTGAGCACACGGCACATCTGGCACGG-5’

3.4. Construction of Radiolabeled DNA Substrates Containing 1st-25mer, U, THF, 8-oxoG, 1nt-Gap and Control

3.4.1. Radiolabeling of oligodeoxynucleotides with ^{32}P

All oligodeoxynucleotides were radiolabeled with [γ-^{32}P]ATP at their 5’-end by using T4 polynucleotide kinase (T4 PNK) reaction seen in Table 5.

Table 5. Radiolabeling reaction of oligodeoxynucleotides with [γ-^{32}P]ATP.

Kinase Reaction	**Volume**	**Final Concentration**
Oligodeoxynucleotide (10 pmol/µl)	1 µl	1 pmol/µl
T4 PNK (20 U)	1 µl	2 U
10X T4 PNK	1 µl	1X
[γ-^{32}P]ATP (10 µCi)	1 µl	1 µCi
dH_2O	6 µl	

The reaction mixture represented in Table 5 was incubated for 1 hour at 37°C. Then the inactivation of kinase reaction was done by increasing the temperature to 65°C and incubating for 20 minutes. After the incubation, the unincorporated [γ-^{32}P]ATP was removed by loading the 10 µl of the reaction mixture onto a Sephadex G-25 column (SigmaAldrich, USA) and centrifuged at 700xg for 1.5 minutes and the 5'-end [γ-^{32}P]ATP-labeled oligodeoxynucleotide eluate was collected (90).

3.4.2. Annealing reaction of radiolabeled DNA substrates containing U, THF, 8-oxoG and Control

For the annealing reaction, 38 µl of dH_2O, 1 µl of 1 M LiCl and 1 µl of 20 pmol/µl complementary oligodeoxynucleotides were added to 10 µl kinase reaction mixture prepared in subheading 3.4.1. The mixture was incubated at 95°C for 5 minutes for substrates containing U, 8-oxoG, and control; for THF-containing substrate, it was incubated at 75°C for 10 minutes. Then the heat block was turned off and let cool at room temperature over a period of 3-4 hours to allow the annealing of the primers. The 5'-end-[γ-^{32}P]ATP-labeled duplex DNA substrates were prepared and stored at 4°C (89).

3.4.3. Annealing reaction of radiolabeled DNA substrate containing 1nt-Gap

For annealing reaction of 1nt-gap oligodeoxynucleotide, two different 25mer oligodeoxynucleotides (1st-25mer and 2nd-25mer) were used. The 1st-25mer oligodeoxynucleotide was radiolabeled with [γ-^{32}P]ATP prior to the annealing reaction (see subheading 3.4.1). To anneal 1nt-Gap oligodeoxynucleotides, 32 µl of dH_2O, 1 µl of 1 M LiCl, 2 µl of 20 pmol/µl complementary oligodeoxynucleotide and 5 µl of 2nd-25mer 10 pmol/µl oligodeoxynucleotide were added to the 10 µl kinase reaction mixture prepared for the 1st-25mer oligodeoxynucleotide. Then, it was incubated at 95°C for 5 minutes and then the heat block was turned off and allowed to cool at room temperature over a period of 3-4 hours for the annealing of the primers. As a result, 5'-end-[γ-^{32}P]ATP-labeled duplex 1 nt-gap DNA substrate was prepared and stored at 4°C (89).

3.5. Construction of Non-radiolabeled DNA Substrates Containing U and 1nt-Gap

To generate non-radiolabeled duplex DNA substrates, 1 µl of oligodeoxynucleotides (10 pmol/µl) were mixed with 9 µl of dH_2O. After generating a 10 µl total mixture; 41 µl of dH_2O, 1 µl of 1 M LiCl, and 1 µl of 20 pmol/µl complementary oligodeoxynucleotides were added to that 10 µl mixture. The mixture was incubated at 95°C for 5 minutes and then the heat block was turned off and let cool at room temperature over a period of 3-4 hours to allow the annealing of the primers. Thanks to this reaction, non-radiolabeled duplex DNA substrates were prepared and they were stored at 4°C (89).

3.6. Measurement of UDG DNA Glycosylase Activity

UDG is a monofunctional DNA glycosylase that recognizes U, U:G, U:A and 5-OH-Ura in the DNA. It cleaves the N-glycosidic bond and leads the formation of an AP site (28,30). To measure the UDG DNA glycosylase activity, the incision experiment was performed. Incision of U was performed in a reaction mixture (10 µl) containing 70 mM HEPES-KOH (pH 7.4), 5 mM EDTA, 1mM DTT, 75 mM NaCl, 10% glycerol and 100 fmol ^{32}P-labeled-U-containing duplex DNA substrate (Table 4 and section 3.4) (91). For optimization, different concentrations (0.25 µg, 0.5 µg and 1 µg) of whole tissue extracts were incubated at 37°C for 30 minutes for initializing of the reactions. For the complete strand cleavage at the AP sites 50 mM NaOH was added and the reactions were terminated by adding 1 volume of 2X formamide stop dye seen in Table 6 and incubating at 75°C for 10 minutes. Then the reactions were ran on 20% 19:1 acrylamide/bis-acrylamide-7 M urea denaturing (PAGE+7M Urea) gel at 15 W for 2 hours in 1X TBE buffer (ThermoFisher, USA). Gels were exposed to PhosphorImager screens (GE HealthCare, USA) overnight at room temperature and visualized by Typhoon PhosphorImager (GE HealthCare, USA). Results were quantitated via ImageQuant software (GE HealthCare, USA). The percentage of incision was calculated as the amount of radioactivity present in the product band relative to the total radioactivity. The 0.25 µg of whole tissue extract was used for the experiments and it was repeated three times.

Table 6. Preparation of 2X formamide stop dye.

Component	Stock Concentration	Volume	Final Concentration
Xylene cyanol	0.5%	60 µl	0.01%
Bromophenol blue	0.2%	150 µl	0.01 %
EDTA	0.5 M	60 µl	10 mM
Formamide	100%	2730 µl	91%

3.7. Measurement of OGG1 DNA Glycosylase Activity

Excision of 8-oxoG from DNA is mainly removed by bifunctional DNA glycosylase, OGG1 (92). To measure OGG1 DNA glycosylase activity, the incision experiment was performed in 10 µl reaction mixture containing 70 mM HEPES-KOH (pH 7.4), 5 mM EDTA, 1 mM DTT, 75 mM KCl, 10% glycerol and 20 fmol ^{32}P-labeled-8-oxoG-containing duplex DNA substrate (91) (Table 4, section3.4). For optimization, different concentrations (0.75 µg and 1.5 µg) of whole tissue extracts were incubated for 30 minutes at 37°C. For the complete strand cleavage of AP sites 50 mM NaOH was added. To terminate the reactions one volume of 2X formamide stop dye was added (Table 6) and incubated at 75°C for 10 minutes. Then the reactions were run on 20% PAGE+7M urea gel at 15 W for 2 hours in 1X TBE buffer (ThermoFisher, USA). Gels were exposed to PhosphorImager screens (GE HealthCare, USA) overnight at room temperature and visualized by Typhoon PhosphorImager (GE HealthCare, USA). Results were quantitated via ImageQuant software (GE HealthCare, USA). The percentage of incision was calculated as the amount of radioactivity present in the product band relative to the total radioactivity. The 1.5 µg of whole tissue extract was selected as the most optimized concentration and all of the samples were repeated for three times in that concentration.

3.8. Measurement of AP Endonuclease Activity

APE1 incises the phosphodiester backbone and causes SSB (30). To measure APE1 activity, the ^{32}P-labeled 51mer duplex DNA substrate with THF at position 26 was used (Table 4, section 3.4). The incision experiment was performed in 10 µl reaction mixture including 50 mM HEPES-KOH (pH 7.4), 25 mM KCl, 0.1 mg/ml BSA, 5 mM $MgCl_2$, 10% glycerol, 0.01% Tween-20 and 50 fmol of ^{32}P-labeled-

THF-containing duplex DNA substrate. For optimization different concentrations (0.5 μg and 0.2 μg) of whole tissue extracts were incubated at 37°C for 15 minutes (91). The reactions were terminated by adding an equal amount of 2X formamide stop dye (Table 6) and incubating at 75°C for 15 minutes. Then the reactions were ran on 20% PAGE+7M urea gel at 15 W for 2 hours 20 minutes in 1X TBE buffer (ThermoFisher, USA). Gels were exposed to PhosphorImager screens (GE HealthCare, USA) overnight at room temperature and visualized by Typhoon PhosphorImager (GE HealthCare, USA). Results were quantitated via ImageQuant software (GE HealthCare, USA). The percentage of incision was calculated as the amount of radioactivity present in the product band relative to the total radioactivity. The 0.2 μg of whole tissue extract was selected as the most optimized concentration and all of the samples were repeated for three times in that concentration.

3.9. Pol β Gap Filling Assay

Pol β is one of the most important core BER enzymes that has an intrinsic dRP lyase activity, which removes the 5'-dRP residue and also it synthesizes one nucleotide to the 3'-end of the existing single-nucleotide gap. The majority of the 5'-dRP lyase activity that exists in the nucleus is come from Pol β (34). To measure Pol β gap-filling activity, the reactions were performed in 10 μl reaction mixture containing 40 mM Tris-HCl (pH 7.4), 5 mM $MgCl_2$, 50 mM KCl, 1 mM DTT, 5 μM dCTP (SigmaAldrich, USA), 5% glycerol, 100 fmol non-radiolabeled-1nt-gap containing duplex DNA substrate at position 26 (Table 4, section 3.4) and 2 μCi of ^{32}P-dCTP (GE HealthCare, USA) (93). For optimization different concentrations (0.125 μg, 0.25 μg and 0.5 μg) of whole tissue extracts were incubated at 37°C for 1 hour for initializing of the reactions. The reactions were terminated by adding an equal amount of 2X formamide stop dye (Table 6) and incubating at 75°C for 10 minutes and then ran on 20% PAGE+7M urea denaturing gel at 15 W for 1 hours and 40 minutes in 1X TBE buffer (ThermoFisher, USA). Gels were exposed to PhosphorImager screens (GE HealthCare, USA) overnight at room temperature and visualized by Typhoon PhosphorImager (GE HealthCare, USA). Results were quantitated via ImageQuant software (GE HealthCare, USA). The percentage of incision was calculated as the amount of radioactivity present in the product band relative to the total radioactivity. The 0.5 μg of whole tissue extract was selected as

the most optimized concentration and all of the samples were repeated for three times in that concentration.

3.10. Whole BER Assay

To measure whole BER capacity in the whole tissue extracts instead of analyzing the BER components one by one, whole BER assay was done. The whole BER assay reactions (10 µl) were done in BER buffer containing 40 mM HEPES (pH 7.6), 0.1 mM EDTA, 5 mM $MgCl_2$, 0.2 mg/ml BSA, 50 mM KCl, 1 mM DTT, 40 mM phosphocreatine, 100 µg/ml creatine phosphokinase, 2 mM ATP, 40 µM of each dATP, dTTP, dGTP and 4 µM of dCTP, 2 µCi of ^{32}P-dCTP (GE HealthCare, USA), 3% glycerol, and 100 fmol of non-radiolabeled-U-containing duplex DNA substrate (93) (Table 4). For optimization different concentrations (0.25 µg and 0.5 µg) of whole tissue extracts were incubated at 37°C for 1 hour for initializing of the reactions. The reactions were terminated by adding an equal amount of 2X formamide stop dye (Table 6) incubating at 75°C for 10 minutes and then ran on 20% PAGE+7M urea gel at 15 W for 2 hours in 1X TBE buffer (ThermoFisher, USA). Gels were exposed to PhosphorImager screens (GE HealthCare, USA) overnight at room temperature and visualized by Typhoon PhosphorImager (GE HealthCare, USA). Results were quantitated via ImageQuant software (GE HealthCare, USA). The percentage of incision was calculated as the amount of radioactivity present in the product band relative to the total radioactivity. The 0.4 µg of whole tissue extract was selected as the most optimized concentration and all of the samples were repeated for three times in that concentration.

3.11. Statistical Analysis

To analyze the differences among NMIBC and corresponding normal tissues, Student's t-test was used and $p<0.05$ was accepted as significant. The tests were two-sided. Analyses were carried out by quantitation of the results via using ImageQuant software and the GraphPad Prism 7 software.

4. RESULTS

4.1. [γ-^{32}P]ATP-labeled DNA Substrates

The [γ-^{32}P]ATP-labeled-1st-25mer single stranded DNA substrate and [γ-^{32}P]ATP-labeled duplex DNA substrates containing U, THF, 8-oxoG, 1nt-gap and control were ran on 12% native polyacrylamide gel at 15 W for 1.40 hours in 1X TBE buffer (ThermoFisher, USA) to check whether the substrates were labeled with [γ-^{32}P]ATP properly, and substrates were annealed correctly or not. Gels were visualized by using Typhoon PhosphorImager (GE HealthCare, USA). As seen in Figure 4, all of the substrates were labeled with [γ-^{32}P]ATP and annealed properly.

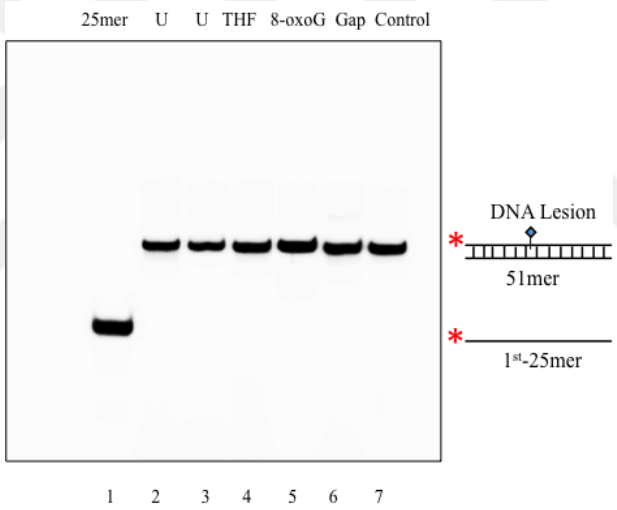

Figure 4. The constructed [γ-^{32}P]ATP-labeled DNA substrates on 12% native polyacrylamide gel. All olideoxynucleotides were 5'-end-[γ-^{32}P]ATP-labeled by T4 PNK. Reaction products were annealed to the complementary strands (except 1st-25mer) by heating the samples except THF-containing substrate at 95°C for 5 minutes (THF-containing substrate at 75°C for 10 minutes) and slowly cooled to room temperature. Lane 1, 1st-25mer single-stranded substrate. Lane 2-3, U-containing 51mer duplex DNA substrate. Lane 4, THF-containing 51mer duplex DNA substrate. Lane 5, 8-oxoG-containing 51mer duplex DNA substrate. Lane 6, 1nt-gap-containing 51mer duplex DNA substrate. Lane 7, 51mer control duplex DNA substrate.

4.2. NMIBC High-Grade Tissues Have Increased UDG DNA Glycosylase Activities

To test whether DNA glycosylase activities are different in NMIBC and corresponding normal tissues, the activity of UDG and OGG1 were measured according to the incision of the [γ-^{32}P]ATP-labeled-oligodeoxynucleotide substrate containing a single lesion U and 8-oxoG, respectively (Table 4, section 3.4). Activity of incision was calculated as the amount of radioactivity in the cleaved band over the total radioactivity. Figure 5 shows the schematic view of DNA glycosylase reaction on denatured PAGE. For example, UDG and OGG1 efficiently incises the double stranded substrates containing U and 8-oxoG at position 26, respectively, and creates the incised product with 25mer as seen in Figure 5. Because the reaction was run on denatured PAGE, [γ-^{32}P]ATP-labeled 25mer single stranded oligodeoxynucleotide are observed in the gel as a cleaved product (Figure 5, lane 2).

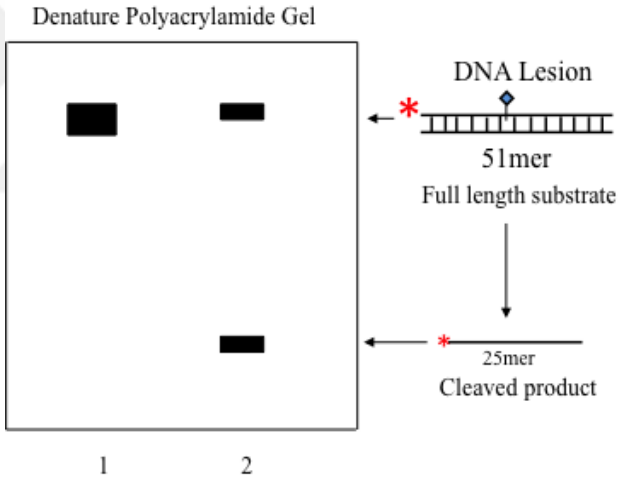

Figure 5. Schematic view of in vitro oligodeoxynucleotide incision assay for DNA glycosylases. The 51mer radiolabeled duplex oligodeoxynucleotide DNA substrate containing a DNA lesion is incised by the appropriate DNA glycosylase that exist in the whole tissue extract and produced a 25mer product. Lane 1, the 51mer radiolabeled duplex oligodeoxynucleotide DNA substrate containing a DNA lesion without tissue extract. Lane 2, the 51mer radiolabeled duplex oligodeoxynucleotide DNA substrate containing a DNA lesion in the presence of tissue extract.

UDG incision assays were performed with increasing concentrations 0.25 μg, 0.5 μg and 1 μg of NMIBC whole tissue protein extracts to identify the optimum protein concentration. UDG efficiently incised the U-containing double stranded 51mer substrate at the single U site at the position 26, generating the 25mer product as expected (Figures 6A and 6B). This experiment showed that UDG activity was increased while the protein concentration increases (Figure 6A, lanes 3-5). It indicates that the measured activity is not contaminated or residual activity in tissue extracts. The 0.25 μg of whole tissue protein extract which shows approximately 60% incision activity was selected as the optimum protein amount for the UDG activity assay (Figure 6A, lane 3). A control (lesion-free) [γ-^{32}P]ATP-labeled-duplex substrate was used as a negative control in each DNA glycosylase assay and no product was observed (Figure 6B, lanes 16, 27 and Figure 7B, lane 16). UDG incision assay for all NMIBC and corresponding normal samples were repeated three times. UDG incision activities were quantified as percentage of incision, and the results were evaluated according to the grades of tissue samples (Figure 6B, 6C and 6D). It was found that no significance difference ($p=0.15$) in the uracil incision activity between low-grade NMIBC tissues and corresponding normal tissues (Figure 6C). However, the uracil incision activity was found significantly higher ($p=0.0001$) in high-grade NMIBC tissues compared with corresponding normal tissues (Figure 6D).

4.3. NMIBC Tissues Have Similar OGG1 DNA Glycosylase Activities

OGG1 incision assays were performed with increasing concentrations (0.75 μg and 1.5 μg) of NMIBC whole tissue protein extracts to determine the optimum protein concentration. It was found that the activity of OGG1 was increased in a concentration-dependent fashion (Figure 7A, lanes 2-3). The 1.5 μg of whole tissue protein extract was selected as the optimum concentration and all NMIBC and corresponding samples were repeated for three times in that concentration to perform OGG1 incision assay. OGG1 efficiently incised the 8-oxoG-containing double stranded 51mer substrate at the single 8-oxoG site at the position 26, generating the expected 25mer product (Figures 7A and 7B). OGG1 incision activities were quantified as percentage of incision, and the results were evaluated according to the grades of tissue samples. As a consequence, for both low- and high-grade NMIBC

and corresponding tissue samples, no significant difference (p=0.942 and p=0.646, respectively) in the percentage of 8-oxoG incision activities was detected (Figure 7C and 7D).

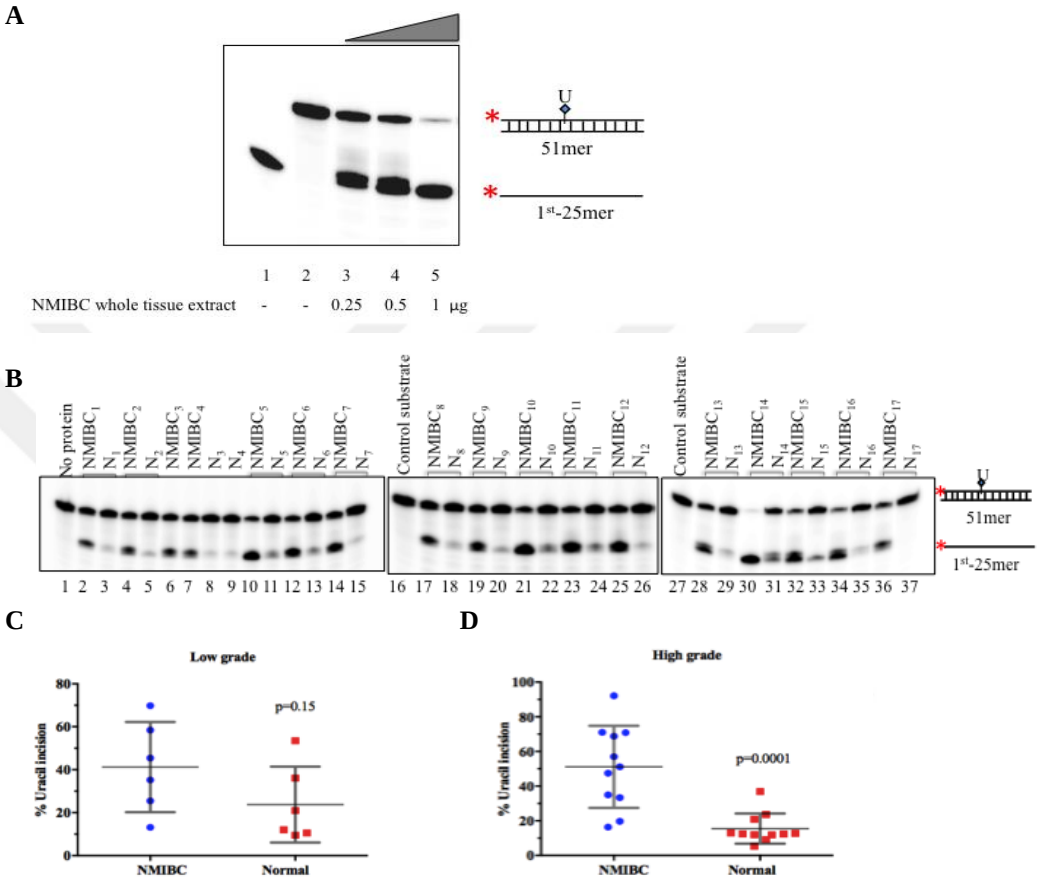

Figure 6. The UDG incision activity on [γ-^{32}P]ATP-labeled duplex substrate containing U in the presence of NMIBC and corresponding normal tissue extracts. Reaction products were ran on a 20% denaturing polyacrylamide gel and visualized by a PhosphorImager. (A) Incision of U-containing [γ-^{32}P]ATP-labeled duplex oligodeoxynucleotide was carried out with; lane 3, 0.25 µg, lane 4, 0.5 µg and lane 5, 1 µg of NMIBC whole tissue extracts. Lane 1, [γ-^{32}P]ATP-labeled-1st-25mer single stranded oligodeoxynucleotide without tissue extract. Lane 2, [γ-^{32}P]ATP-labeled duplex DNA substrate containing U without tissue extract. (B) Incision of the [γ-^{32}P]ATP-labeled duplex U-containing substrate was carried out 0.25 µg of NMIBC and corresponding normal tissue extracts. Lane 1, [γ-^{32}P]ATP-labeled duplex DNA substrate containing U without tissue extract. Lanes 16 and 27, [γ-^{32}P]ATP-labeled duplex DNA control substrate with tissue extract. Lanes 3-15, and lanes 17-26 and lanes 28-37 the incision activity of NMIBC and corresponding normal tissue samples. Percentage of U incision activities of (C) low-grade (D) high-grade NMIBC and corresponding normal tissue extracts. The percentage of incision activity is calculated as the amount of radioactivity present in the product band relative to the total radioactivity.

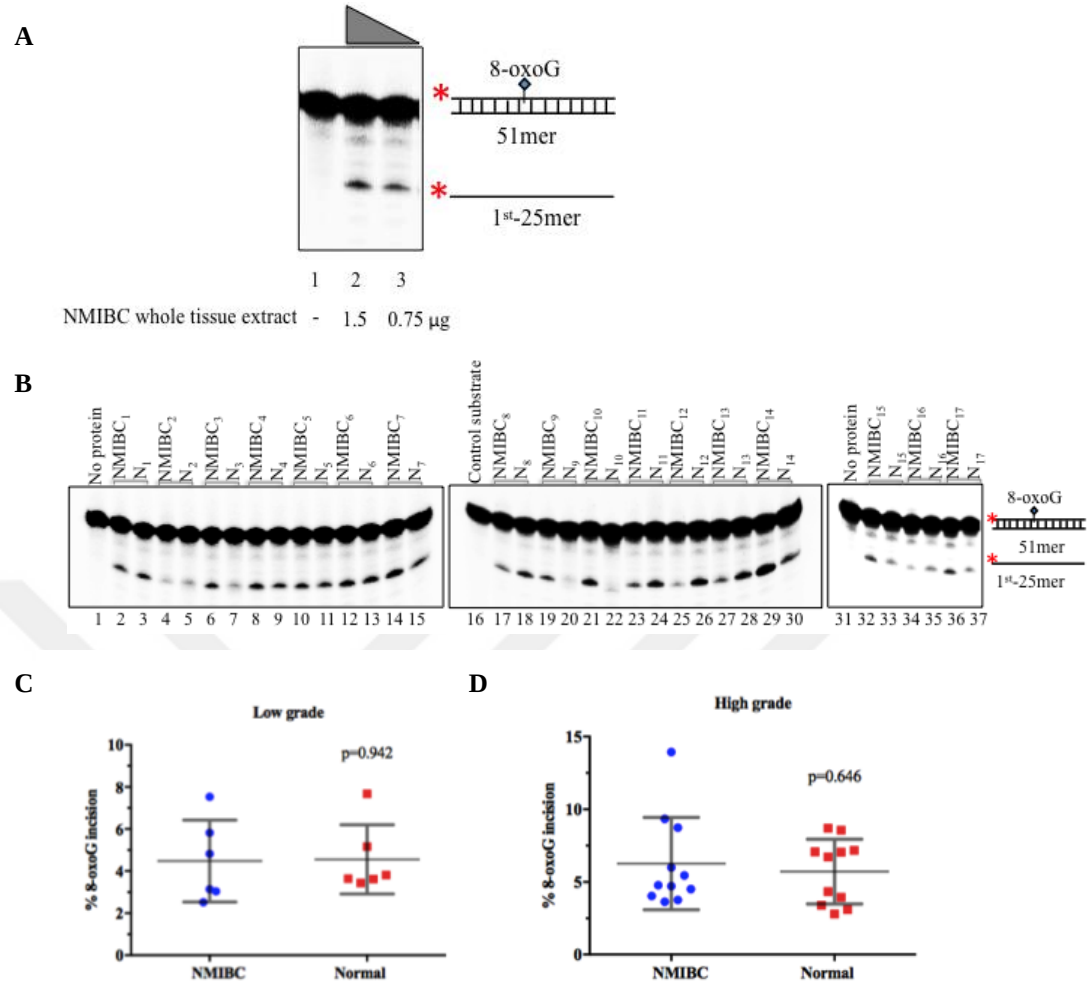

Figure 7. The OGG1 incision activity on [γ-^{32}P]ATP-labeled duplex substrate containing 8-oxoG in the presence of NMIBC and corresponding normal tissue extracts. Reaction products were ran on a 20% denaturing polyacrylamide gel and visualized by a PhosphorImager. (A) Incision of 8-oxoG-containing γ-^{32}P]ATP-labeled duplex oligodeoxynucleotide was carried out with increasing concentrations (0.75 and 1.5 µg; lanes 3 and 2 respectively) of NMIBC whole tissue extracts. Lane 1, [γ-^{32}P]ATP-labeled duplex DNA substrate containing 8-oxoG without tissue extract. (B) Incision of [γ-^{32}P]ATP-labeled duplex 8-oxoG-containing substrate was carried out 1.5 µg of NMIBC and corresponding normal tissue extracts. Lanes 1 and 31, [γ-^{32}P]ATP-labeled duplex DNA substrate containing 8-oxoG without tissue extract. Lane 16, [γ-^{32}P]ATP-labeled duplex DNA control substrate with tissue extract. Lanes 2-15, lanes 17-30 and lanes 32-37, incision activity of NMIBC and corresponding normal tissue extracts. Percentage of 8-oxoG incision activities of (C) low-grade (D) high-grade NMIBC and corresponding normal tissue extracts. The percentage of incision is calculated as the amount of radioactivity present in the product band relative to the total radioactivity.

4.4. Both Low- and High-Grade NMIBC Tissues Have Increased APE1 Activity

The activity of APE1 that exists in whole tissue extracts of NMIBC and corresponding normal tissues was measured by using an AP site counterpart THF-DNA substrate (Table 4, section 3.4). THF site is cleaved by APE1, however it cannot be cut by bifunctional DNA glycosylases, such as OGG1 (Figure 8) (16).

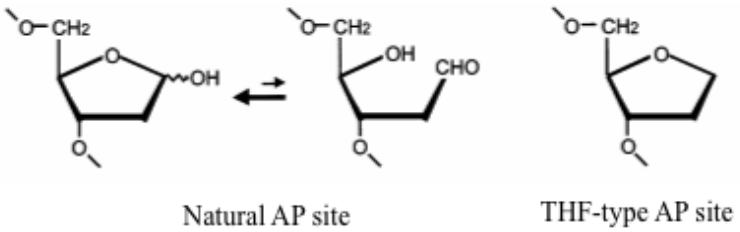

Figure 8. Natural and THF AP sites structures (94).

THF-incision assays were performed with increasing concentrations (0.2 μg and 0.5 μg) of whole tissue protein extracts to determine the optimum protein concentration and it was found that the activity of APE1 was increased in a protein concentration-dependent fashion. (Figure 9A, lanes 3-4). The 0.2 μg of whole tissue protein extract was selected as the optimum protein concentration and all NMIBC and corresponding normal tissue extracts were repeated for three times in that concentration to perform THF incision assay. A control (lesion-free) [γ-^{32}P]ATP-labeled-duplex substrate was used as a negative control in APE1 activity assay and no product was formed (Figure 9B, lanes 15, 29). It was determined that APE1 efficiently cleaved the THF-containing duplex 51mer substrate at the single THF site at the position 26 and generated the expected 25mer product (Figures 9A and 9B). AP site incision activities were quantified as the percentage of incision, and the results were evaluated according to the grades of tissue samples. As a result, APE1 activity was found significantly higher in both low- ($p=0.026$) and high-grade ($p<0.0001$) NMIBC than corresponding tissue samples as seen in Figures 9C and 9D. In addition, it was found that AP-site incision activities of NMIBC tissue samples were higher than low-grade samples (Figures 9C and 9D).

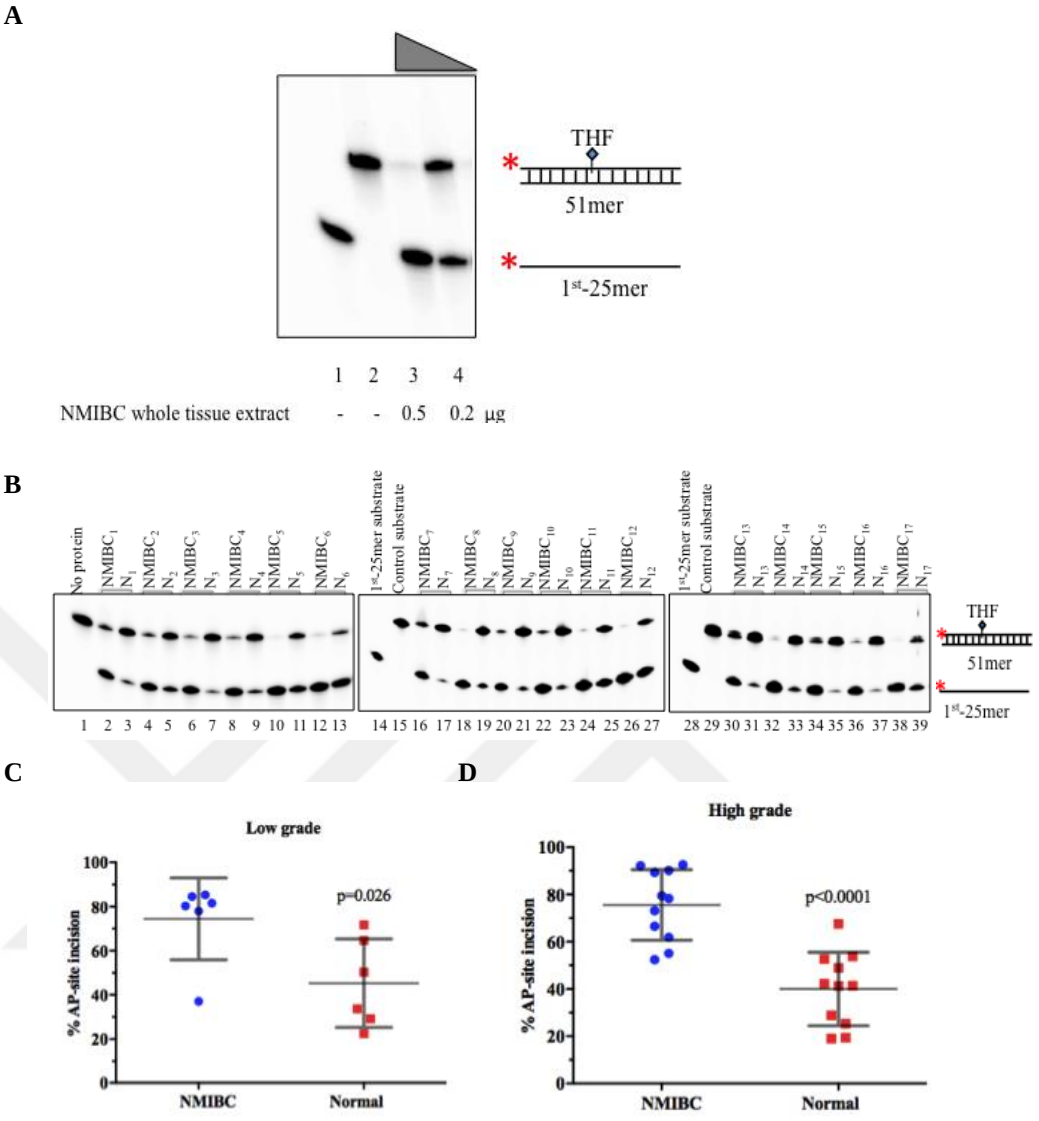

Figure 9. The APE1 activity on [γ-^{32}P]ATP-labeled duplex DNA substrate with THF in the presence of NMIBC and corresponding normal tissue extracts. Reaction products were ran on a 20% denaturing polyacrylamide gel and visualized by a PhosphorImager. (A) Incision of THF-containing [γ-^{32}P]ATP-labeled duplex DNA substrate was carried out with increasing concentrations (0.5 and 0.2 µg; lanes 3 and 4, respectively) of NMIBC whole tissue extracts. Lane 1, [γ-^{32}P]ATP-labeled-1st-25mer single stranded oligodeoxynucleotide without tissue extract. Lane 2, [γ-^{32}P]ATP-labeled duplex DNA substrate containing THF without tissue extract. (B) Incision of [γ-^{32}P]ATP-labeled duplex THF-containing DNA substrate was carried out 0.2 µg of NMIBC and corresponding normal tissue extracts. Lane 1 [γ-^{32}P]ATP-labeled duplex DNA substrate containing THF without tissue extract. Lane 14 and 28, the [γ-^{32}P]ATP-labeled-1st-25mer single stranded oligodeoxynucleotide. Lanes 15 and 29, [γ-^{32}P]ATP-labeled duplex DNA control substrate with tissue extract. Lanes 2-13, lanes 16-27, and lanes 30-39, AP site incision activities of NMIBC and corresponding normal tissue extracts. Percentage of AP site incision activities of (C) low-grade (D) high-grade NMIBC and corresponding normal tissue extracts. The percentage of incision is calculated as the amount of radioactivity present in the product band relative to the total radioactivity.

4.5. NMIBC High-Grade Tissues Have Increased Pol β Activities

To test whether Pol β activity is altered in NMIBC and corresponding normal tissues, the activity of single nucleotide gap filling that is the ^{32}P-dCTP nucleotide incorporation into a 51mer duplex DNA substrate containing 1nt-gap at position 26 was measured (Figure 10).

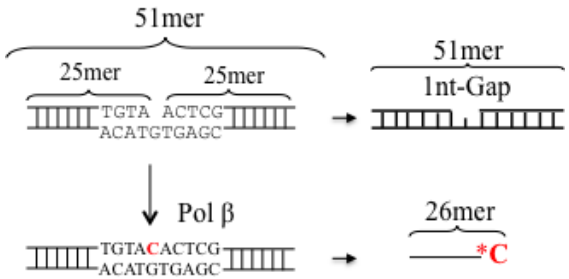

Figure 10. The schematic view of one nucleotide incorporation of Pol β. The gap at position 26 of 51mer non-radiolabeled duplex oligodeoxynucleotide is efficiently filled by Pol β, producing a 26mer product.

Pol β incorporated ^{32}P-dCTP at position 26 of the 51mer substrate and generated a product with 26mer as seen in Figures 11A and 11B. At the beginning, the assay was performed using 0.125 μg, 0.25 μg and 0.5 μg of whole tissue lysates of NMIBC and the corresponding normal tissues to determine the optimum protein concentration (Figure 11A). The 0.5 μg of whole tissue protein extract was selected as the optimum protein concentration and all NMIBC and corresponding normal tissue extracts were repeated for three times in that concentration to perform Pol β single nucleotide incorporation assay. It was determined that Pol β efficiently incorporates the ^{32}P-dCTP to the 1nt-gap site and generated a 26mer product (Figures 11A and 11B). The gap filling activities of Pol β were quantified as relative ^{32}P-dCTP incorporation with PhosphorImager units and the results were evaluated by considering the grades of the tissue samples. As a consequence, for low-grade NMIBC and corresponding samples, no significant difference ($p=0.348$) was detected in relative ^{32}P-dCTP incorporation activities of Pol β (Figure 11C). There is a significant difference between high grade-NMIBC samples and corresponding normal tissues, $p= 0.041$ (Figure 11D).

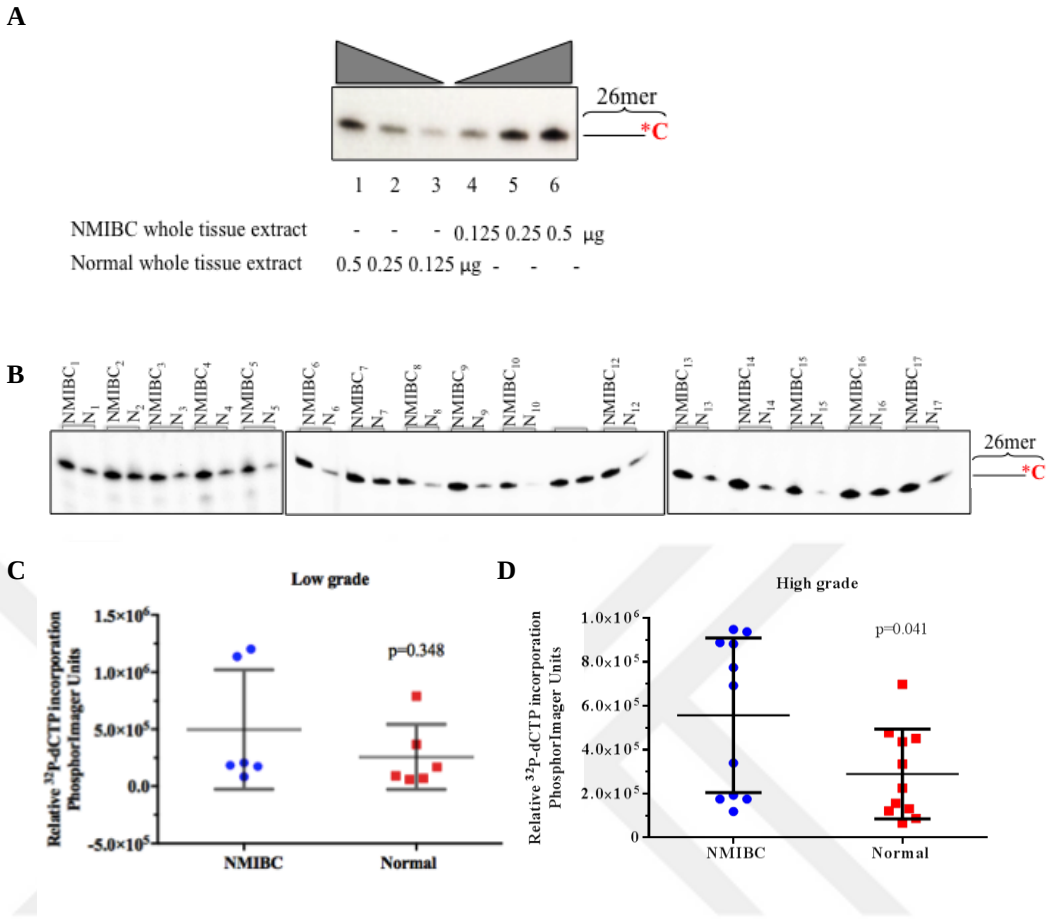

Figure 11. The one nucleotide (^{32}P-dCTP) incorporation activity of Pol β on non-radiolabeled duplex substrate containing 1 nt-gap at position 26 in the presence of NMIBC and corresponding normal tissue extracts. Reaction products were ran on a 20% denaturing polyacrylamide gel and visualized by a PhosphorImager. (A) Incorporation of a single ^{32}P-dCTP into a 51mer duplex substrate containing 1nt-gap at position 26 was carried out with increasing concentrations (0.5, 0.25 and 0.125 µg; lanes 1, 2 and 3, respectively) of normal whole tissue extracts (lanes 4-6) of NMIBC whole tissue extracts. (B) Incorporation of a single ^{32}P-dCTP into a 51mer duplex substrate containing 1nt-gap at position 26 was carried out 0.5 µg of NMIBC and corresponding normal tissue extracts. Relative ^{32}P-dCTP incorporation of (C) low-grade (D) high-grade NMIBC and corresponding normal tissue extracts. The gap filling activities of Pol β were quantified as relative ^{32}P-dCTP incorporation with PhosphorImager units.

4.6. NMIBC High-Grade Tissues Have Increased Whole BER Capacity

Uracil-initiated BER capacity in NMIBC and corresponding normal tissues was determined as both ^{32}P-dCTP nucleotide incorporation into a non-radiolabeled 51mer duplex DNA substrate with U/G at position 26, and subsequent ligation of the incorporated product. It was expected that UDG recognizes the existing U in the substrate, leaving an AP site for APE1 to make 3'-OH for Pol β and Pol β fills the one nucleotide gap and the nick is ligated by LigIII and XRCC1 complex as seen in Figure 12.

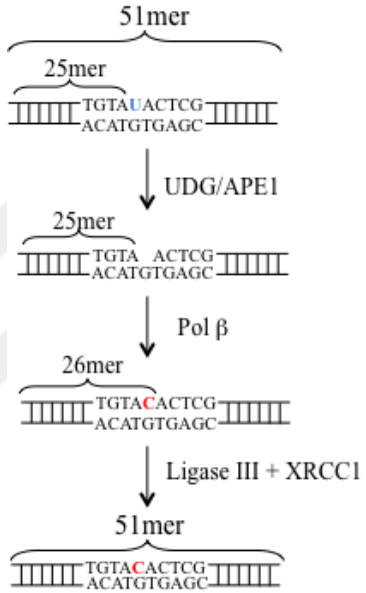

Figure 12. In vitro whole BER process. The U at position 26 of 51mer non-radiolabeled duplex substrate is recognized by UDG and further processed by APE1 to allow Pol β's one nucleotide incorporation and lastly the nick is sealed by Ligase III and XRCC1 complex resulting with a 51mer product.

At the beginning, the assay was performed using 0.25 μg and 0.5 μg of whole tissue lysates of NMIBC and the corresponding normal tissues to determine the optimum protein concentration (Figure 13A). The 0.4 μg of whole tissue protein extract was selected as the optimum protein concentration (Figure 13A, lane 2). All NMIBC and corresponding normal tissue extracts were repeated for three times in that concentration to perform whole BER assay. It was determined that the U which exists in the non-radiolabeled 51mer duplex DNA substrate was efficiently incised and further processed, and then Pol β efficiently incorporates the ^{32}P-dCTP to the

1nt-gap site and generated a 26mer product (Figure 13B, lower band). It was also detected that subsequent to incorporation of ^{32}P-dCTP, the product was ligated efficiently and 51mer product was generated (Figure 13B, upper band). The ^{32}P-dCTP incorporation and ligation activities were quantified as relative ^{32}P-dCTP incorporation with PhosphorImager units and the results were evaluated by considering the grades of the tissue samples. It was found that no significance difference ($p=0.13$) in the incorporation of a ^{32}P-dCTP between low-grade NMIBC and corresponding tissues (Figure 13C). However, ^{32}P-dCTP incorporation activities were found significantly higher ($p=0.048$) in high-grade NMIBC tissues compared with corresponding tissues (Figure 13D). On the other hand, ligation product activity was found significantly higher in both low ($p=0.026$) and high-grade ($p=0.002$) NMIBC than corresponding tissue samples as seen in Figures 13E and 13F.

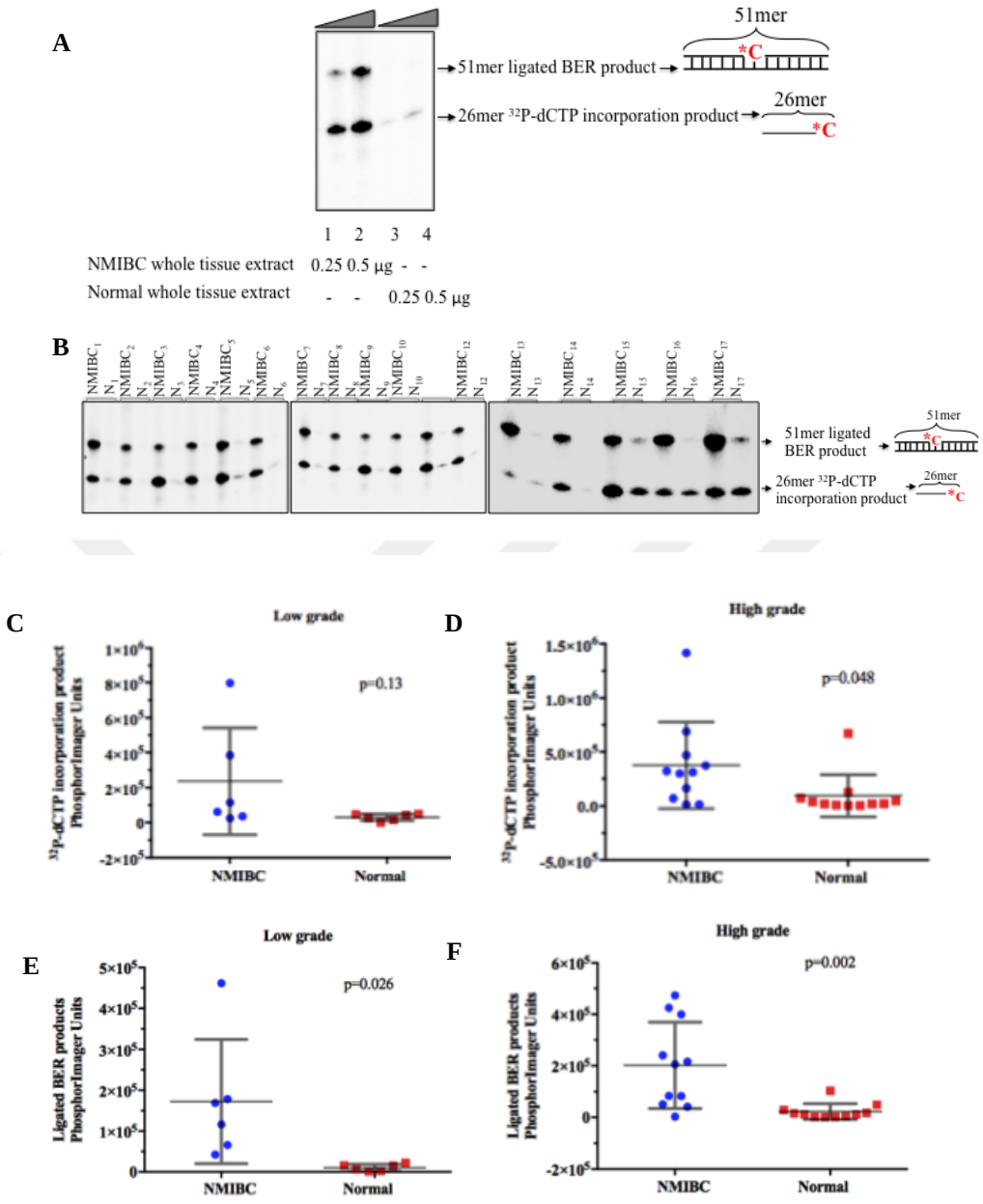

Figure 13. U-initiated BER capacity in NMIBC and corresponding normal tissues by using a non-radiolabeled 51mer duplex substrate with U/G at position 26. Reaction products were ran on a 20% denaturing polyacrylamide gel and visualized by a PhosphorImager. (A) Incorporation of a single ^{32}P-dCTP into a 51mer duplex substrate containing U at position 26 and subsequent ligation of incorporated product were carried out with increasing concentrations (0.25 and 0.5 µg; lanes 1 and 2, respectively) of NMIBC whole tissue extracts and increasing concentrations (0.25 and 0.5 µg; lanes 3 and 4, respectively) of normal whole tissue extracts. (B) Incorporation of a single ^{32}P-dCTP into a 51mer duplex substrate containing U at position 26 and subsequent ligation of incorporated product were carried out 0.4 µg of NMIBC and corresponding normal tissue extracts. Relative ^{32}P-dCTP incorporation of (C) low-grade (D) high-grade, and ligated BER products activity of (E) low-grade (F) high-grade NMIBC and corresponding normal tissue extracts.

4.7. Inter-individual Variations in BER

All of the analyzed facts (UDG, OGG1, APE1, Pol β and whole BER capacity) were evaluated as inter-individual variations to understand personalized therapy approaches. In the case of U incision activity, out of seventeen normal tissue extracts of individuals; one of them showed less than 10%, ten of them showed ~10%, three of them showed ~20%, two of them showed ~40%, and one of them showed ~50% U incision activities (Figure 14A). In addition to the different percentages of U incision activities of normal tissue extracts, individuals NMIBC tissues also showed different percentages of activities as follows: one of them showed ~10%, two of them showed ~20%, one of them showed ~30%, three of them showed ~40%, three of them showed ~50%, two of them showed ~60%, four of them showed ~70%, and one person showed ~90% U incision activities (Figure 14A). For 8-oxoG incision activity, out of seventeen normal tissue extracts of individuals; seven of them showed less than 5%, three of them showed ~5%, and seven of them showed ~8% 8-oxoG incision activities (Figure 14B). Also their NMIBC tissues also showed different percentages of activities as follows: three of them showed less than ~5%, ten of them showed ~5%, one of them showed ~8%, two of them showed ~10%, and one person showed ~15% 8-oxoG incision activities (Figure 14B). For AP site incision activity, out of seventeen normal tissue extracts of individuals; seven of them showed 50%, three of them showed ~70%, four of them showed ~20%, and three of them showed ~30% AP site incision activities (Figure 14C). Besides corresponding normal tissue extracts, inter-individual differences occur for NMIBC tissue extracts of seventeen individuals as follows: one person showed ~40%, two of them showed ~50%, three of them showed ~70%, seven of them showed ~80%, and four people showed ~90% AP site incision activities (Figure 14C). In the case of Pol β's gap filling activity, out of seventeen normal tissue extracts of individuals; twelve of them showed less than $5.0x10^5$ units, two of them showed ~ $5.0x10^5$, and three of them showed between $5.0x10^5$ and $1.0x10^6$ relative ^{32}P-dCTP incorporation activities as PhosphorImager units (Figure 14D). Individuals NMIBC tissue extracts Pol β's gap filling activities were differed as follows: nine people showed less than $5.0x10^5$, two of them showed between $5.0x10^5$ and $1.0x10^6$, four of them showed ~$1.0x10^6$, and two of them showed ~$1.25x10^6$ relative ^{32}P-dCTP incorporation activities as

PhosphorImager units (Figure 14D). In the case of whole BER activity according to ^{32}P-dCTP incorporation activities, out of seventeen normal tissue extracts of individuals; except two individual, the others showed almost zero ^{32}P-dCTP incorporation activities as PhosphorImager units (Figure 14E). However, each individual's NMIBC tissue extract showed variable value of ^{32}P-dCTP incorporation activity between 0.0 and ~1.5x10^{6} PhosphorImager units (Figure 14E). Whole BER activity was also analyzed as the subsequent ligation of the BER products. Out of seventeen normal tissue extracts of individuals; each of person showed different value of ligation activity which most of them were close to zero PhosphorImager units (Figure 14F). Although each individual's normal tissue showed almost zero activity as PhosphorImager units except two people; individuals NMIBC tissue extracts ligation activities were differed between 0 and 6x10^{5} PhosphorImager units (Figure 14F).

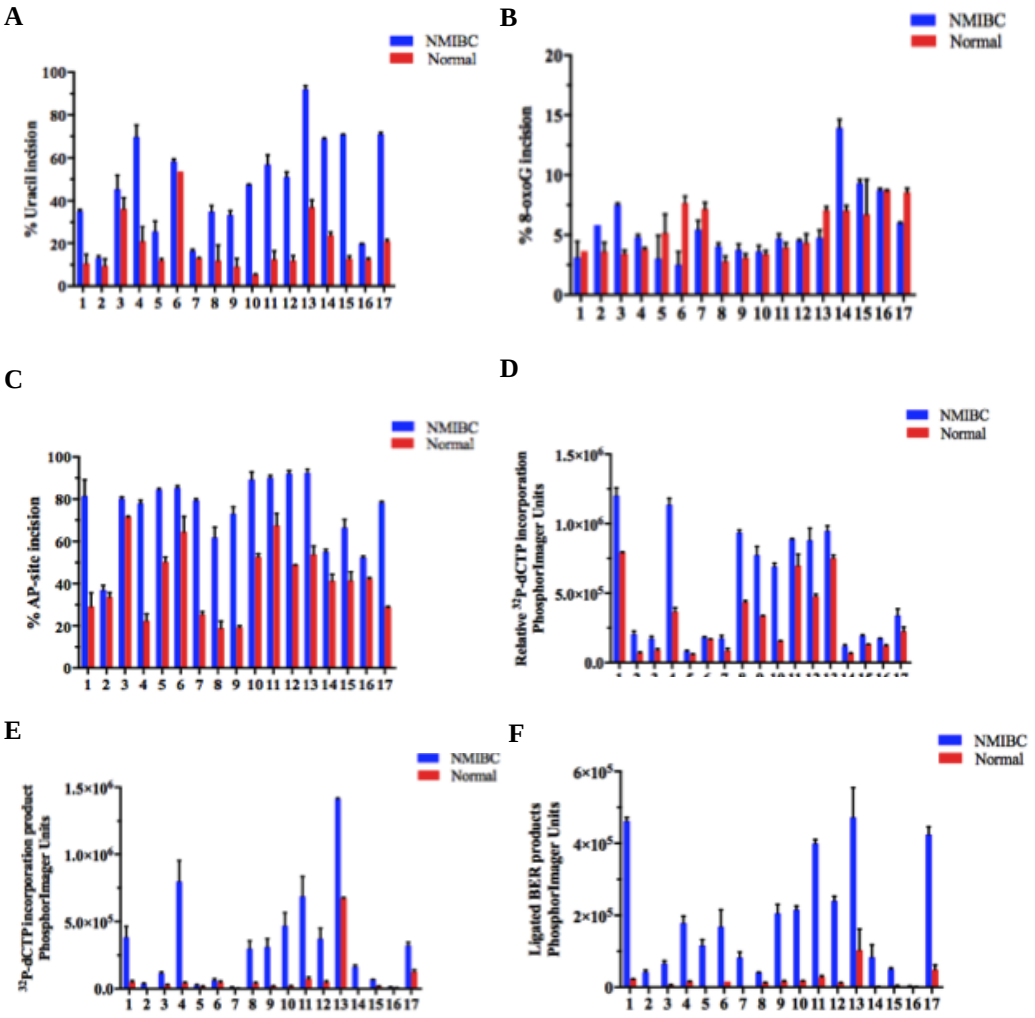

Figure 14. Inter-individual variations in NMIBC and corresponding normal tissue extracts. Inter-individual variations in NMIBC and corresponding normal tissue extracts. (A) Uracil incision. (B) 8-oxoG incision. (C) AP-site incision. (D) Relative ^{32}P-dCTP incorporation. (E) ^{32}P-dCTP incorporation product of U-initiated whole BER assay. (F) Subsequent ligated BER products of U-initiated whole BER assay.

5. DISCUSSION AND CONCLUSION

The unrepaired DNA damage is one of the most important factors that cause carcinogenesis. It promotes accumulation of mutations and genomic instability, hence, induces cancer development (28,49). The most common malignancy of the urinary tract is BC (95). The mechanism involved in the development of BC has still not been understood. It is suggested that accumulation of toxins occur in bladder during excretion and these toxins generate further carcinogenic by-products that give rise to DNA damage and thus carcinogenesis occurs (3,4). The majority of BCs at diagnosis involve NMIBC (95). Especially, NMIBC patients with high-grade tumors show enhanced recurrence risk, and to prevent recurrence and metastasis several chemotherapeutic agents or BCG are used as an adjuvant therapy following TUR of bladder tumor (5,6,95). These therapies show their cytotoxic effect by causing alkylated, oxidized and deaminated DNA damages, and SSBs (6,7,8) which are repaired by BER pathway (9). Since insufficient BER capacity leads to carcinogenesis while extreme BER capacity leads to development of drug resistance, therefore the balance of BER capacity in cells is very important to maintain genomic integrity and stability (10). Therefore, it is important to investigate NMIBC in the context of BER capacity to understand cancer susceptibility, progression, and responses to chemotherapy, to develop predictive, prognostic and therapeutic biomarkers, and for personalized therapy. The role of BER capacity in NMIBC has still not been known. Thus, the goal of this thesis is to determine total BER capacity as well as the activities of key BER proteins including UDG, OGG1, APE1 and Pol β in tumors and corresponding normal tissues of NMIBC patients. The results demonstrate that high-grade NMIBC is associated with a significantly increased total BER capacity as well as increased UDG, APE1 and Pol β activities. Moreover, this study clearly shows the inter-individual variations in the BER capacity of normal and NMIBC tissues.

The BER is started with DNA glycosylases, which recognize and cut out the damaged base. Previous studies demonstrated that alterations in the expression levels or activity of major DNA glycosylases such as UDG and OGG1 were relevant to drug resistance or cancer progression including lung, head, neck and colorectal

cancers (54-57). However, their role in NMIBC is not known yet. Therefore in this study, the activities of UDG and OGG1 were measured in whole tissue lysates of NMIBC and corresponding normal tissues. As UDG and OGG1 are the primary DNA glycosylases which remove U and 8-oxoG lesions from DNA, respectively, their activities were measured as the incision of double stranded oligodeoxynucleotide substrates containing a single U or 8-oxoG lesions (Table 4) in NMIBC and corresponding normal tissue extracts. In this study, it was found that U incision activity was significantly higher in high-grade NMIBC tissues compared with corresponding normal tissues while there was no significant difference between low-grade samples (Figures 6C and 6D). Recently, Wei et al demonstrated that rs3890995 in *UDG* gene was associated with NMIBC progression in patients receiving BCG treatment (81). It was suggested that rs3890995 in *UDG* gene might affect its transcription and protein level and thus might affect the activity of UDG, thereby contributing the progression in NMIBC as seen in high-grade tumors. On the other hand, no significant differences in the 8-oxoG incision activities were detected in this study for both low- and high-grade NMIBC and corresponding tissue samples (Figures 7C and 7D). The recent meta-analysis (82) reported no significant relation between *OGG1* gene polymorphisms and BC risk that supports this finding.

APE1 is one of the key enzymes that play a role in BER. In several studies, it has been demonstrated that APE1 is overexpressed in a great deal of cancer types such as prostate, breast, triple-negative breast, colon, ovarian, non-small cell lung, head and neck squamous cancers (55,56,59-64). The overexpression of APE1 is associated with resistance to chemotherapy and radiotherapy whereas down regulation or inhibition of APE1 function increase sensitivity of a variety of anticancer drugs (53,61-65). The elevated levels of APE1/Ref-1 protein were found in serum and urine of NMIBC and MIBC patients, indicating the importance of APE1 function in bladder cancer therapy (86,87). Also, a recent study has been indicated that high-grade tumors of NMIBC and MIBC patients showed increased levels of APE1 (85). However, the identified expression and protein levels are not directly reflecting the activity of APE1 in NMIBC. Therefore, this study was investigated for the first time, the activity of APE1 in NMIBC and corresponding normal tissue extracts by using a THF-containing double stranded

oligodeoxynucleotide substrate (Table 4). In this study, it was found that both low- and high-grade NMIBC tissue extracts had increased APE1 activity compared to corresponding normal tissue extracts (Figures 9C and 9D). Additionally, it was observed that AP-site incision activities of high-grade NMIBC tissue samples were higher than low-grade ones (Figures 9C and 9D). The increased expression and protein levels of APE1, which was shown in previous studies, are correlated with the elevated APE1 activity and the severity of NMIBC observed in this study. Thus, APE1 bears a potential to act as a prognostic biomarker as well as a therapeutic biomarker in context of choosing the treatment approach to minimize drug resistance.

The main DNA polymerase, which plays role in BER, is Pol β. Aberrant forms and overexpression of Pol β has been identified in too many cancer types involving breast, ovarian, colon, prostate, esophageal and colorectal cancers (66-71). For BC case, a few variants of Pol β were identified (67) and one SNP, rs3136717, of Pol β was associated with higher BC risk (9). Another recent study has been demonstrated that high-grade tumors of NMIBC and MIBC patients showed increased levels of Pol β in compared to low grade ones (85). However, the identified expression levels and different forms of Pol β do not reflect its exact activity. Thus, in this study the activity of Pol β in NMIBC and corresponding tissue extracts was investigated by measuring single nucleotide gap filling activity on 1nt-gap containing double stranded oligodeoxynucleotide substrate (Figure 11). In this study, it was found that single nucleotide gap filling activity of Pol β was significantly higher in high-grade NMIBC tissues compared with corresponding normal tissues while there was no significant difference between low-grade samples (Figures 11C and 11D). The increased Pol β expression levels in high-grade tumors of NMIBC and MIBC patients, which were shown in a previous study (85), are correlated with increased Pol β activity in high-grade tumors of NMIBC patients. It was suggested that rs3136717 in *Pol β* gene might affect its transcription and thus might affect Pol β activity, for that reason contributing NMIBC progression.

Because alterations in BER capacity can influence both cancer progression and responses to chemotherapy and radiotherapy, it is crucial to determine the capacity of total BER pathway in different types of cancer (96). In this study,

although the key BER enzymes activities, UDG, OGG1, APE1 and Pol β, were measured one by one, their results may not accurately reflect the total BER capacity of NMBIC tissues, because they may not be the regulatory steps of BER pathway. For NMIBC, the overall BER capacity has been not determined yet. Therefore, uracil initiated total BER capacity in NMIBC and corresponding normal tissues was analyzed as both ^{32}P-dCTP nucleotide addition into a non-radiolabeled duplex DNA substrate (Table 4) and subsequent ligation of the incorporated product. In this study, it was found that high-grade NMIBC tissues demonstrate significantly higher ^{32}P-dCTP incorporation and ligation activities than their corresponding normal tissues (Figures 13D and 13F) whereas low-grade ones only showed significant increase in the ligation product activity (Figure 13E). The results indicate that NMIBC has increased overall BER capacity. Although low-grade NMIBC tissue extracts demonstrated significant increase in ligation activity, the increase in high-grade NMIBC tissue extracts was higher. The finding that total BER capacity positively correlated with the condition of UDG, APE1 and Pol β in high-grade NMIBC tissue extracts supports the notion that increased total BER capacity was caused by the increased activity of these three enzymes. In addition, the increased ligation activity of high-grade NMIBC tumor extracts found in this study is consistent with the study demonstrating that increased levels of XRCC1 were associated with high-grade tumors of NMIBC and MIBC (85). Thus, these findings suggest that the increased in BER capacity of NMIBC due to increased UDG, APE1 and/or Pol β activities can enhance the chemotherapeutic resistance to NMIBC and contribute to progression of NMIBC.

Each individual has different DNA repair capacity and efficacy (97). DNA repair capacity is a term that consists of several facts such as SNPs, gene expression, stability and function of gene products as well as lifestyle and environmental conditions (98). Some of the cancer cells are inherently resistant to DNA damaging therapeutics, while the resistance during therapy is more common for most of the cancer cells (99). Therefore, determining DNA repair capacity is crucial for choosing the optimum therapy that minimizes the side effects of therapies and provides maximum benefit to patients. Since therapies involved in NMIBC are related with BER pathway, this study also investigated the inter-individual variations in BER

capacity according to UDG, OGG1, APE1, Pol β and whole BER activity. In this study, it was found that each patient's normal and NMIBC tissue showed different UDG, 8-oxoG, APE1, Pol β and overall BER capacity from each other (Figure 14). Additionally, an obvious difference in UDG capacity was observed between high-grade NMIBC tumors and corresponding normal tissues (Figure 14A). The increased UDG capacity may associate with the severity of NMIBC. In addition to UDG capacity, a remarkable increase of APE1 capacity was detected in most of the patients regardless of the tumor grade (Figure 14C). Thus, APE1 and/or UDG may act as a therapeutic biomarker(s) to predict and choose the most beneficial treatment strategy. Another noteworthy point is that the observation of the extreme increases of overall BER capacity in most of the patients NMIBC tumor tissues rather than their corresponding normal samples regardless of the tumor grade (Figures 14E and 14F). This condition is highlighting the role of enhanced BER capacity in NMIBC patients. All in all, determining each patient's own BER capacity will provide the selection of most beneficial therapy option by predicting cancer cells reaction to treatment of NMIBC patients.

In conclusion, in the present study the activities of key BER proteins and overall BER capacity in NMIBC patients' tumors and their corresponding normal tissues were investigated. These results demonstrate that the elevated overall BER capacity due to increased UDG, APE1 and/or Pol β activities is associated with high-grade NMIBC. Furthermore, this thesis emphasizes the inter-individual variations occurring in BER capacity. All these facts contribute to the personalized therapy approaches within the scope of developing predictive, prognostic and therapeutic biomarkers to provide maximum benefit to NMIBC patients.

REFERENCES

1. Antoni S, Ferlay J, Soerjomataram I, Znaor A, Jemal A, Bray F. Bladder cancer incidence and mortality: A global overview and recent trends. European Urology 2017; 71(1):96-108
2. Knowles MA, Hurst CD. Molecular biology of bladder cancer: New insights into pathogenesis and clinical diversity. Nature Reviews Cancer 2015; 15(1):25-41
3. Wang G, Abrams J, Wang L, Xu XS. Histone deacetylases (HDACS) in XPC gene silencing and bladder cancer. Journal of Hematology & Oncology 2011; 4(17):1-11
4. Smolensky D, Rathore K, Cekanova M. Molecular targets in urothelial cancer: Detection, treatment, and animal models of bladder cancer. Drug Design, Development and Theraphy 2016; 10:3305-3322
5. Chang JS, Lara PN, Pan C. Progress in personalizing chemotherapy for bladder cancer. Advances in Urology 2012; 1-10
6. Martínez-Fernández M, Rubio C, Segovia C, López-Calderón FF, Dueñas M, Paramio JM. EZH2 in bladder cancer, a promising therapeutic target. Int J Mol Sci 2015; 16(11):27107-27132
7. Cheung-Ong K, Giaever G, Nislow C. DNA-damaging agents in cancer chemotherapy: Serendipity and chemical biology. Chem Biol 2013; 20(5):648-659
8. Shah G, Zielonka J, Chen F, Zhang G, Cao Y, Kalyanaraman B, See W. H_2O_2 generation by BCG induces the cellular oxidative stress response required for BCG's direct effects on urothelial carcinoma tumor biology. J Urol 2014; 192(4):1238-1248
9. Xie H, Gong Y, Dai J, Wu X, Gu J. Genetic variations in base excision repair pathway and risk of bladder cancer: A case-control study in the United States. Mol Carcinog 2015; 54(1):50-57
10. Jalal S, Earley JN, Turchi JJ. DNA repair: From genome maintenance to biomarker and therapeutic target. Clin Cancer Res 2011; 17(22):6973-6984
11. Compérant E, Varinot J, Moroch J, Eymerit-Morin C, Brimo F. A practical guide to bladder cancer pathology. Nat Rev Urol 2018; 15(3):143-154
12. Shulz WA. Molecular Biology of Human Cancers. Dordrecht, Springer, 2007: p.18-19
13. Miyamoto H, Brimo F, Schultz L, Ye H, Miller JS, Fajardo DA, Lee TK, Epstein JI, Netto GJ. Low-grade papillary urothelial carcinoma of the urinary bladder. Arch Pathol Lab Med 2010; 134:1160-1163

14. Pierro GB, Gluia C, Cristini C, Fraietta G, Marini L, Grande P, Gentile V, Piergentili R. Bladder cancer: A simple model becomes complex. Current Genomics 2012; 13(5):395-415
15. Ye F, Wang L, Castillo-Martin M, McBride R, Galsky MD, Zhu J, Bofetta P, Zhang DY, Cordon-Cardo C. Biomarkers for bladder cancer management: Present and future. Am J Clin Exp Urol 2014; 2(1):1-14
16. Hedge ML, Mantha AK, Hazra TK, Bhakat KK, Mitra S, Szczesny. Oxidative genome damage and its repair: Implications in aging and neurodegenerative diseases. Mech Ageing Dev 2012; 133(4):157-168
17. Maynard S, Fang EF, Scheibye-Knudsen M, Croteau DL, Bohr VA. DNA damage, DNA repair, aging and neurodegeneration. Cold Spring Harb Perspect Med 2015; 5(10):a025130
18. Hakem R. DNA-damage repair; the good, the bad, and the ugly. The EMBO Journal 2008; 27(4):589-605
19. Dexheimer TS. Cabarcas S, Hurt E. (Eds) DNA Repair of Cancer Stem Cells. Dordrecht, Springer, 2013: p.19-32
20. Christmann M, Tomicic MT, Roos WP, Kaina B. Mechanisms of human DNA repair: An update. Toxicology 2003; 193(1-2):3-34
21. Bont RD, Larebeke NV. Endogenous DNA damage in humans: A review of quantitative data. Mutagenesis 2004; 19(3):169-185
22. Evans MD, Dizdaroglu M, Cookea MS. Oxidative DNA damage and disease: Induction, repair and significance. Mutation Research 2004; 567(1):1-61
23. Scott TL, Rangaswamy S, Wicker CA, Izumi T. Repair of oxidative DNA damage and cancer: Recent progress in DNA base excision repair. Antioxid Redox Signal 2014; 20(4):708-726
24. Chakarov S, Petkova R, Russev GC, Zhelev N. DNA damage and mutation. Types of DNA damage. Biodiscovery 2014; 11:e8957
25. Allgayer J, Kitsera N, Lippen C, Epe B, Khobta A. Modulation of base excision repair of 8-oxoguanine by the nucleotide sequence. Nucleic Acids Research 2013; 41(18):8559-8571
26. Abbotts R, Thompson N, Madhusudan S. DNA repair in cancer: Emerging targets for personalized therapy. Cancer Management and Research 2014; 6(1):77-92
27. Ambekar SS, Hattur SS, Bule PB. DNA: Damage and repair mechanisms in humans. Glob J Pharmaceu Sci 2017; 3(2):001-007
28. Wallace SS. Base excision repair: A critical player in many games. DNA Repair 2014;

19:14-26

29. Krokan HE, Bjørås M. Base excision repair. Cold Spring Harb Perspect Biol 2013; 5(4):1-22
30. Whitaker AM, Schaich MA, Smith MS, Flynn TS, Freudenthal BD. Base excision repair of oxidative DNA damage: From mechanism to disease. Front Biosci 2017; 22:1493-1522
31. Schermerhorn KM, Delaney S. A chemical and kinetic perspective on base excision repair of DNA. Acc Chem Res 2014; 47(4):1238-1246
32. Wilson III DM, Bohr VA. The mechanics of base excision repair, and its relationship to aging and disease. DNA Repair 2007; 6(4):544-559
33. Prakash A, Doublié S. Base excision repair in the mitochondria. J Cell Biochem 2015; 116(8):1490-1499
34. Sykora P, Kanno S, Akbari M, Kulikowicz T, Baptiste BA, Leandro GS, Lu H, Tian J, May A, Becker KA, Croteau DL, Wilson III DM, Sobol RW, Yasui A, Bohr VA. DNA polymerase beta participates in mitochondrial DNA Repair. Mol Cell Biol 2017; 37(16):1-20
35. Kim YJ, Wilson III DM. Overview of base excision repair biochemistry. Curr Mol Pharmacol 2012; 5(1):3-13
36. Jacobs AL, Schär P. DNA glycosylases: In DNA repair and beyond. Chromosoma 2012; 121(1):1-20
37. Gredilla R, Bohr VA, Stevnsner T, Danish Center for Molecular Gerontology and Danish Aging Research Center. Mitochondrial DNA repair and association with aging-an update. Exp Gerontol 2010; 45(7-8):478-488.
38. Souzo-Pinto NC, Wilson III DM, Stevnsner TV, Bohr VA. Mitochondrial DNA,base excision repair and neurodegeneration. DNA Repair 2008; 7(7):1098-1109
39. Fritz G. Human APE1/Ref-1 protein. Int J Biochem Cell Biol 2000; 32:925-929
40. Dyrkheeva NS, Khodyreva SN, Lavrik OI. Multifunctional human apurinic/apyrimidinic endonuclease 1: Role of additional functions. Molecular Biology 2007; 41(3):402-416
41. Tell G, Damante G, Caldwell D, Kelley MR. The intracellular localization of APE1/Ref-1: More than a passive phenomenon?. Antioxidants & Redox Signaling 2005; 7(3-4):367-384
42. Kladova O, Bazlekowa-Karaban M, Baconnais S, Pietrement O, Ishchenko AA, Matkarimov BT, Fedorova OS, Le Cam E, Tudek B, Kuznetsov NA, Saparbaev M. The role of the N-terminal domain of human apurinic/apyrimidinic endonuclease 1, APE1, in DNA glycosylase stimulation. DNA Repair 2018; 64:10-25

43. Li M, Wilson III DM. Human apurinic/apyrimidinic endonuclease 1. Antioxidants & Redox Signaling 2014; 20(4):678-707
44. Wong D, DeMott MS, Demple B. Modulation of the 3′→5′-exonuclease activity of human apurinic endonuclease (Ape1) by its 5′-incised abasic DNA product. J Biol Chem 2003; 278(38):36242-36249
45. Wilson SH, Beard W. Structure and mechanism of DNA polymerase β. Biochemistry 2014; 53:2768-2780
46. Chyan Y-J, Ackerman S, Shepherd NS, McBride OW, Widen SG, Wilson SH, Wood TG. The human DNA polymerase β gene structure. Evidence of alternative splicing in gene expression. Nucleic Acids Research 1994; 22(14):2719-2715
47. Idriss HT, Al-Assar O, Wilson SH. DNA polymerase β. Int J Biochem Cell Biol 2002; 34(4):321-324
48. Wilson SH, Beard WA, Shock DD, Batra VK, Cavanaugh NA, Prasad R, Hou EW, Liu Y, Asagoshi K, Horton JK, Stefanick DF, Kedar PS, Carrozza MJ, Masaoka A, Heacock ML. Base excision repair and design of small molecule inhibitors of human DNA polymerase β. Cell Mol Life Sci 2010; 67(21):3633-3647
49. Torgovnick A, Schumacher B. DNA repair mechanisms in cancer development and therapy. Front Genet 2015; 6(157)
50. Kelley MR, Fishel ML. DNA repair proteins as molecular targets for cancer therapeutics. Anticancer Agents Med Chem 2008; 8(4):417-425
51. Tell G, Wilson III DM. Targeting DNA repair proteins for cancer treatment. Cell Mol Life Sci 2010; 67(21):3569-3572
52. Nickoloff JA, Jones D, Lee S-H, Williamson EA, Hromas R. Drugging the cancers addicted to DNA repair. J Natl Cancer Inst 2017; 109(11):1-13
53. Dianov GL. Base excision repair targets for cancer therapy. Am J Cancer Res 2011; 1(7):845-851
54. Dizdaroglu M, Jaruga P. Oxidatively induced DNA damage and cancer. J Mol Biomark Diagn 2011; 01(S2):1-13
55. Mahjabeen I, Ali K, Zhou X, Kayani MA. Deregulation of base excision repair gene expression and enhanced proliferation in head and neck squamous cell carcinoma. Tumor Biol 2014; 35(6):5971-5983
56. Obtulowicz T, Swoboda M, Speina E, Gackowski D, Rozalski R, Siomek A, Janik J, Janowska B, Ciesla M, Jawien A, Banaszkiewicz Z, Guz J, Dziaman T, Szpila A, Olinski R, Tudek B. Oxidative stress and 8-oxoguanine repair are enhanced in colon adenoma and carcinoma patients. Mutagenesis 2010; 25(5):463-471

57. Weeks LD, Zentner GE, Scacheri PC, Gerson SL. Uracil DNA glycosylase (UNG) loss enhances DNA double strand break formation in human cancer cells exposed to pemetrexed. Cell Death and Disease 2014; 5(2):e1045-10
58. Mei W, Zunzhen Z, Wangjun C. Suppression of a DNA base excision repair gene, hOGG1, increases bleomycin sensitivity of human lung cancer cell line. Toxicology and Applied Pharmacology 2008; 228(3):395-402
59. Juhnke M, Heumann A, Chirico V, Höflmayer D, Menz A, Hinsch A, Hube-Magg C, Kluth M, Lang DS, Möller-Koop C, Sauter G, Simon R, Beyer B, Pompe R, Thederan I, Schlomm T, Luebke AM. Apurinic/apyrimidinic endonuclease 1 (APE1/Ref-1) overexpression is an independent prognostic marker in prostate cancer without TMPRSS2: ERG fusion. J Med Virol 2017; 1:1-26
60. Curtis CD, Thorngren DL, Nardulli AM. Immunohistochemical analysis of oxidative stress and DNA repair proteins in normal mammary and breast cancer tissues. BMC Cancer 2010; 10(1):1-13
61. Zhang Y, Wang J, Xiang D, Wang D, Xin X. Alterations in the expression of the apurinic/apyrimidinic endonuclease-1/redox factor-1 (APE1/Ref-1) in human ovarian cancer and identification of the therapeutic potential of APE1/Ref-1 inhibitor. Int J Oncol 2009; 35(5):1069-1079
62. Chen T, Liu C, Lu H, Yin M, Shao C, Hu X, Wu J, Wang Y. The expression of APE1 in triple-negative breast cancer and its effect on drug sensitivity of olaparib. Tumor Biology 2017; 39(10):1-9
63. Wen X, Lu R, Xie S, Zheng H, Wang H, Wang Y, Sun J, Gao X, Guo L. APE1 overexpression promotes the progression of ovarian cancer and serves as a potential therapeutic target. Cancer Biomarkers 2016; 17(3):313-322
64. Wang D, Xiang D, Yang X, Chen L, Li M. APE1 overexpression is associated with cisplatin resistance in non-small cell lung cancer and targeted inhibition of APE1 enhances the activity of cisplatin in A549 cells. Lung Cancer 2009; 66(3):298-304
65. Kelley MR, Logsdon D, Fishel ML. Targeting DNA repair pathways for cancer treatment: What's new? Future Oncol 2015; 10(7):1215-1237
66. Salehan MR, Morse HR. DNA damage repair and tolerance: a role in chemotherapeutic drug resistance. Br J Biomed Sci 2013; 70(1):31-40
67. Starcevic D, Dalal S, Sweasy JB. Is there a link between DNA polymerase β and cancer. Cell Cycle 2004; 3(8):996-999
68. Albertella MR, Lau A, O'Connor MJ. The overexpression of specialized DNA polymerases in cancer. DNA repair 2005; 4(5):583-593

69. Iwatsuki M, Mimori K, Yokobori T, Tanaka F, Tahara K, Inoue H, Baba H, Mori M. A platinum agent resistance gene, POLB, is a prognostic indicator in colorectal cancer. J Surg Oncol 2009; 100(3):261-266
70. Bergoglio V, Canitrot Y, Hogarth L, Minto L, Howell SB, Cazaux C, Hoffmann J. Enhanced expression and activity of DNA polymerase β in human ovarian tumor cells: Impact on sensitivity towards antitumor agents. Oncogene 2001; 20:6181-6187
71. Hong Z, Peng X, Min L, Jimin Z, Ziming D, Guoqiang Z. DNA polymerase beta expression correlates with poor prognosis in esophageal cancer patients. Chin Sci Bull 2013; 58(26):3274-3279
72. Simonelli V, Leuzzi G, Basile G, D'Errico M, Fortini P, Franchitto A, Viti V, Brown AR, Parlanti E, Pascucci B, Palli D, Giuliani A, Palombo F, Sobol RW, Dogliotti E. Crosstalk between mismatch repair and base excision repair in human gastric cancer. Oncotarget 2017; 8(49):84827-84840
73. Illuzzi JL, Wilson III DM. Base excision repair: Contribution to tumorigenesis and target in anticancer treatment paradigms. Curr Med Chem 2012; 19(23):3922-3936
74. Mouw KW. DNA repair pathway alterations in bladder cancer. Cancers 2017; 9(4):1-14
75. Bellmunt J, Paz-Ares L, Cuello M, Cecere FL, Albiol S, Guilem V, Gallardo E, Carles L, Mendez P, Cruz JJ, Taron M, Rosell R, Baselga J. Gene expression of ERCC1 as a novel prognostic marker in advanced bladder cancer patients receiving cisplatin-based chemotherapy. Ann Oncol 2007; 18(3):522-528
76. Van Allen EM, Mouw KW, Kim P, Iyer G, Wagle N, Al-Ahmadie H, Zhu C, Ostrovnaya I, Kryukov GV, O'Connor KW, Sfakianos J, Garcia-Grossman I, Kim J, Guancial EA, Bambury R, Bahl S, Gupta N, Farlow D, Qu A, Signoretti S, Barletta JA, Reuter V, Boehm J, Lawrence M, Getz G, Kantoff P, Bochner BH, Choueiri TK, Bajorin DF, Solit DB, Gabriel S, D'Andrea A, Garraway LA, Rosenberg JE. Somatic ERCC2 mutations correlate with cisplatin sensitivity in muscle-invasive urothelial carcinoma. Cancer Discov 2014; 4(10):1140-1153
77. Li J, Zhang J, Liu Y, Ye G. Increased expression of DNA repair gene XPF enhances resistance to hydroxycamptothecin in bladder cancer. Med Sci Monit 2012; 18(4):BR156-162
78. Wang D, Feng J-F, Yuan G-Y, Yang Y-H, Liu Y-S, Yang Y-W. Association between chromosomal aberration of exfoliated bladder cells in the urine and oxidative stress in patients with bladder transitional cell carcinoma. Oncol Lett 2017; 14(1):137-144
79. Zhang F, Wu J-H, Zhao W, Liu H-T. XRCC1 polymorphisms increase bladder cancer risk in Asians: A meta analysis. Tumor Biol 2013; 34(5):2659-2664

80. Mittal RD, Mandal RK, Gangwar R. Base excision repair pathway genes polymorphism in prostate and bladder cancer risk in North Indian population. Mech Ageing Dev 2012; 133(4):127-132
81. Wei H, Kamat A, Chen M, Ke H-L, Chang DW, Yin J, Grossman HB, Dinney CP, Wu X. Association of polymorphisms in oxidative stress genes with clinical outcomes for bladder cancer treated with Bacillus Calmette-Guérin. PLoS One 2012; 7(6):e38533
82. Wenjuan C, Jianzhong L, Chong L, Yanjun G, Keqing L, Hanzhang W, Zhiping W. The hOGG1 Ser326Cys gene polymorphism and susceptibility for bladder cancer: A meta-analysis. Int Braz J Urol 2016; 42(5):883-896
83. Gossage L, Perry C, Abbotts R, Madhusudan S. Base excision repair factors are promising prognostic and predictive markers in cancer. Curr Mol Pharmacol 2012; 5(1):115-124
84. Sak SC, Harnden P, Johnston CF, Paul AB, Kiltie AE. APE1 and XRCC1 protein expression levels predict cancer-specific survival following radical radiotherapy in bladder cancer. Clin Cancer Res 2005; 11(17):6205-6211
85. Chantre-Justino M, Alves G, Britto C, Cardoso A, Scherrer L, Moreire AS, Quirino R, Ornellas A, Leitão A, Lage C. Impact of reduced levels of APE1 transcripts on the survival of patients with urothelial carcinoma of the bladder. Oncol Rep 2015; 34(4):1667-1674
86. Shin JH, Choi S, Lee YR, Park MS, Na YG, Irani K, Lee SD, Park JB, Kim JM, Lim JS, Jeon BH. APE1/Ref-1 as a serological biomarker for the detection of bladder cancer. Cancer Res Treat 2015; 47(4):823-833
87. Choi S, Shin JH, Lee YR, Joo HK, Song KH, Na YG, Chang SJ, Lim JS, Jeon BH. Urinary APE1/Ref-1: A potential bladder cancer biomarker. Dis Markers 2016; 2016:1-8
88. Bergkvist A, Ljungqvist A, Moberger G. Classification of bladder tumours based on the cellular pattern. Preliminary report of a clinical-pathological study of 300 cases with a minimum follow-up of eight years. Acta Chir Scand 1965; 130(4):371-378
89. Aamann MD, Hvitby C, Popuri V, Muftuoglu M, Lemminger L, Skeby CK, Keijzers G, Ahn B, Bjørås M, Bohr VA, Stevnsner T. Cockayne syndrome group B protein stimulates NEIL2 DNA glycosylase activity. Mech Ageing Dev 2014; 135:1-14
90. Souza-Pinto NC, Croteau DL, Hudson EK, Hansford RG, Bohr VA. Age-associated increase in 8-oxodeoxyguanosine glycosylase/AP lyase activity in rat mitochondria. Nucleic Acids Research 1999; 27(8):1935-1942
91. Muftuoglu M, Souza-Pinto NC, Dogan A, Aamann M, Stevnsner T, Rybanska I, Kirkali

G, Dizdaroglu M, Bohr VA. Cockayne syndrome group B protein stimulates repair of formamidopyrimidines by NEIL1 DNA glycosylase. J Biol Chem 2009; 284(14):9270-9279

92. Fortini P, Pascucci B, Parlanti E, D'Errico M, Simonelli V, Dogliotti E. 8-Oxoguanine DNA damage: At the crossroad of alternative repairpathways. Mutation Research 2003; 531(1-2):127-139
93. Maynard S, Souza-Pinto NC, Scheibye-Knudsen M, Bohr VA. Mitochondrial base excision repair assays. Methods 2010; 51(4):416-425
94. Otsuka C, Sanadai S, Hata Y, Okuto H, Noskov VN, Loakes D, Negishi K. Difference between deoxyribose- and tetrahydrofuran-type abasic sites in the in vivo mutagenic responses in yeast. Nucleic Acids Research 2002; 30(23):5129-5135
95. Anastasiadis A, Reijke TM. Best practice in the treatment of nonmuscle invasive bladder cancer. Ther Adv Urol 2012; 4(1):13-32
96. Weissman L, Jo D-G, Sørensen MM, Souzo-Pinto NC, Markesbery WR, Mattson MP, Bohr VA. Defective DNA base excision repair in brain from individuals with Alzheimer's disease and amnestic mild cognitive impairment. Nucleic Acids Research 2007; 35(16):5545-5555
97. Vergne Y, Matta J, Morales L, Vargas W, Alvarez-Garriga C, Bayona M. Breast cancer and DNA repair capacity: Association with use of multivitamin and calcium supplements. Integr Med (Encinitas) 2013; 12(3):38-46
98. Slyskova J, Naccarati A, Polakova V, Pardini B, Vodickova L, Stetina R, Schmuczerova J, Smerhovsky Z, Lipska L, Vodicka P. DNA damage and nucleotide excision repair capacity in healthy individuals. Environ Mol Mutagen 2011; 52:511-517
99. Nagel ZD, Kitange GJ, Gupta SK, Joughin BA, Chaim IA, Mazzucato P, Lauffenburger DA, Sarkaria JN, Samson LD. DNA repair capacity in multiple pathways predicts chemoresistance in glioblastoma multiforme. Cancer Research 2017; 77(1):198-206

CURRICULUM VITAE

Personal Information

Name	Fatma Merve	**Surname**	ANTMEN
Place of Birth	Istanbul	**Date of birth**	02.07.1994
Nationality	Turkish Republic	**Telephone number**	+905333582802
E-mail	mtansev@gmail.com		

Education

Level	Institution Name	Graduate Year
Master	Mehmet Ali Aydınlar Acibadem University	2018
Undergraduate	Istanbul Bilgi University	2016
High School	FMV Private Erenköy Işık Science High School	2012

Work Experience

Position	Corporation	Duration
Research Assistant	Acıbadem Mehmet Ali Aydınlar University	08.2016-
Laboratory Intern	Memorial Ataşehir Hospital, IVF Andrologia and Genetics Center	07.2015-08.2015
Laboratory Intern	Yeditepe University Hospital Genetics Diagnose Center	06.2014-07.2014

Foreign Languages

Language	Reading	Speaking	Writing
English	Advanced	Advanced	Advanced
French	Elementary	Elementary	Elementary

***** Evaluated as advanced, good, intermediate, beginner

Foreign Language Exam Results [#]

YDS	YÖK-DİL	IELTS	TOEFL IBT	TOEFL PBT	TOEFL CBT	FCE	CAE	CPE
77,5	86,25							

[#] All successful exams should be enrolled.

[#] YDS: Yabancı Dil Sınavı; YÖK-Dil: Yükseköğretim Kurumları Yabancı Dil Sınavı; IELTS: International English Language Testing System; TOEFL IBT: Test of English as a Foreign Language-Internet-Based Test TOEFL PBT: Test of English as a Foreign Language-Paper-Based Test; TOEFL CBT: Test of English as a Foreign Language-Computer-Based Test; FCE: First Certificate in English; CAE: Certificate in Advanced English; CPE: Certificate of Proficiency in English

Other Exams

Name of the Exam	Quantitative	Equally Weighted	Verbal
ALES**	68,9	70,1	66,7

ALES:** Akademik Personel ve Lisansüstü Eğitimi Giriş Sınavı

Computer Skills

Program	Ability to Use
MS Office	Advanced
MacOS	Advanced
MATLAB	Beginner
R Studio	Beginner

***** Evaluated as advanced, good, intermediate, beginner

Projects

Name of the Project	Institution	Position	Years
Development of the original 2-indolinone compounds as anti-interleukin 1 and chemotherapeutic drugs Sub-project 2: DNA repair inhibitors to be developed as a new drug for the treatment of hereditary nonpolyposis colorectal cancer (MLH1 gene defect). TUBITAK 1003, Project No: 215S614	Acıbadem Mehmet Ali Aydınlar University	Research Scholar	11.2016-07.2018
Determination of Small Molecule Inhibitors Blocking Mitochondrial Base Repairing Mechanism and Their Activities by Targeting DNA Polymerase Gamma Enzyme for Cancer Therapy. TUBITAK 1001, Project No: 212T026	Acıbadem Mehmet Ali Aydınlar University	Research Scholar	08.2016-11.2016
Senior Design Graduation Project: Detection of the Expression Level of SnoN and TGF-β Proteins in T-ALL Cell Lines and Human Thymus	Istanbul Bilgi University	Researcher	2015-2016
Science High School Graduation Project: Fermented Turnip Juices Effects on Food Poisoning's Bacteria and Human Stomach	Yeditepe University	Researcher	2011-2012
TUBITAK-BİDEB Inter-regional Competition of Research Projects in High School Students: Examination of Fisheries and Examination of Fishermen's Problems in Manyas and Uluabat Lakes	FMV Private Erenköy Işık Science High School	Researcher	2009-2010

Scholarships and Awards

Explanation	Institution	Years
MSc. Program of Medical Biotechnology, 100% Scholarship	Acıbadem Mehmet Ali Aydınlar University	2016-2018
BSc. Program of Genetics and Bioengineering, additional 50% Achievement Scholarship	Istanbul Bilgi University	2014-2015
Istanbul Bilgi University, Genetics and Bioengineering, 50% Achievement Scholarship	ÖSYS	2012-2016
The Secondariness Award in Geography	TÜBİTAK-BİDEB	2009-2010

Conferences and Courses

	Position	Institution	Duration
Genome Maintenance, DNA Repair and Cancer	Organization committee and participant	Acıbadem Mehmet Ali Aydınlar University	26-28.04.2018
Training Course on the Use of Experimental Animals	Participant	Acıbadem Mehmet Ali Aydınlar University	14-30.10.2016
Nanotechnology and Tissue Engineering: Current Challenges & Future Prospects	Participant	Istanbul Kültür University	12.2014 (9 hours)
BioForm	Participant	Yıldız Technical University	11.2014 (6 hours)

Presentations and Abstracts

Name of the Abstract	Explanation
Enhanced Apurinic/Apyrimidinic Endonuclease Activity in Non-Muscle Invasive Bladder Cancer	36th World Congress of Endourology, Paris, 20 – 23 September 2018

International and National Certificates

Name	Institution	Year
Certificate of Experimental Animal Use	Acıbadem Mehmet Ali Aydınlar University	2016
Certificate of Participation to Nanotechnology and Tissue Engineering: Current Challenges & Future Prospects	Istanbul Kültür University	2014
Certificate of Participation to BioForm	Yıldız Technical University	2014
The Secondariness Achievement Certificate in Geography	TUBITAK-BİDEB	2009-2010